

QC
AVRO
Rept
GEN/1090/336





A. V. ROE CANADA LIMITED
MALTON - ONTARIO

TECHNICAL DEPARTMENT (Aircraft)

AIRCRAFT:

REPORT NO. Gen/1090/336

FILE NO:

NO. OF SHEETS: 85

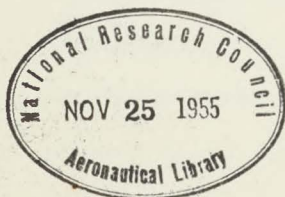
TITLE:

4 Front page, ect.
60 Main text.
21 Appendix.

THEORY of MULTI-SPAR and MULTI-RIE
WING STRUCTURES.

This paper makes obsolete the following Reports:

Gen/1090/329-330-331-332.



PREPARED BY Alex. Grzedzielski DATE June 1955

CHECKED BY _____ DATE _____

SUPERVISED BY _____ DATE _____

APPROVED BY J. H. Mitchell DATE Aug 1955

ISSUE NO.	REVISION NO.	REVISED BY	APPROVED BY	DATE	REMARKS
2					4 pages added to the Appendix.
3					renumbering of figures 17 on.

THEORY of MULTI-SPAR and MULTI-RIB
WING STRUCTURES

Alex. Grzedzielski, P.Eng, Dr.Eng.
Senior Stress Engineer, Avro Aircraft Ltd.

SUMMARY

A Method of stress and deflection analysis of low aspect ratio wings is presented, proceeding entirely with redundant stress distributions. The effects of wing sweep, taper, lateral contraction, and torsional warping are correctly accounted for. The method presumes the use of a high speed digital computer.

- I) Introduction
- II) Outline of the Method
- III) Arithmetic Operations
- IV) Examples
- V) Appendix
- Acknowledgement
- References

I. INTRODUCTION

The stress analysis of high aspect ratio subsonic wings was a development of the beam theory, and although the primitive bending stress distribution had to be corrected, most of the times, by warping and shear lag distributions, the whole analysis was basically one dimensional with the span coordinate as independent variable. With the advent of the low aspect ratio supersonic wing, the analysis has become a chapter of the theory of plates and, therefore, a two dimensional problem. In these wings, stress distribution is defined in terms of two local bending moments acting at different angles and of a local torque, all three depending on span and chord coordinates. Thus computations grew extremely involved and tedious, and quite hopeless without an electronic computing machine.

There are two possible ways of approach. One is through determination of displacements, the other through redundant distributions of plate bending and torque moments. In the first method, displacements of selected wing points, at spar and rib intersections for instance, are assumed as unknown quantities. Then, either the stress components are expressed in terms of these unknowns and substituted in the equilibrium conditions, or better, the strain energy of the structure is found in terms of the unknowns and the virtual work theorem is applied. In either case a large set of linear simultaneous equations is obtained, connecting the unknown displacements with the known acting loads. The pro-

cedure is known as the method of influence coefficients.

In the second method, at first an approximative moment distribution is assumed so as to satisfy the equilibrium conditions exactly, but leaving strains still incompatible. Then, the assumed distribution is corrected by several properly chosen self-equilibrated groups of internal loads. Their magnitude is determined from the Castigliano theorem, again by solving a large set of linear equations. Subsequently, the stress distribution is determined and, if desired, displacements are computed by the dummy load method.

In practice, the two methods are complementary rather than alternative. The first one is best suited if the object of computation is to establish displacements as functions of the applied load, i.e. in aero-elasticity and in flutter analysis. However, the method is not adequate for detail stressing. It is common knowledge that quite a crude assumption concerning the stress distribution yields displacements which favorably compare with experiment. Hence, a method designed so as to be acceptable for aero-elastic purposes with the least number of unknowns, does not provide sufficient information for stress analysis. But the difficulty lies deeper. According to Ref.(3) Part 1, Chapter IV, 4.1, even an exact solution of the plate theory, when given in terms of displacements, may not, if at all, produce stresses with acceptable accuracy. If so, what accuracy can one hope to obtain from a method using finite differences, in terms depending on third or fourth differences? The

displacement method, does not yield stress distribution as a byproduct. On the other hand, a method satisfactory for detail stressing may be too laborious for aeroelasticity.

This paper intends to contribute to the stressing method of low aspect ratio wings, and proceeds entirely with redundant stress distributions. The roots of the expounded technique are in the paper of Yuan-Cheng Fung, Ref.(2), however many vital features have been added and the applications are much wider. The method accounts correctly for taper and sweep effects, for Poisson's ratio, for torsional warping, and for the shear lag effect. It is designed so that the bulk of arithmetic operations is performed by high speed digital computing machines.

II. OUTLINE OF THE METHOD

1. Preliminary Remarks

The usual hypothesis in the analysis of thick skin, multi-spar/rib structures is known as the lumping method. Accordingly, when considering wing bending, skin material is thought to be accumulated along spar and rib flanges, and it is left in its place when considering wing torsion. Clearly, the hypothesis is admissible, although it neglects the effects of lateral contraction, (Poisson's ratio) and seemingly yields good results for straight wings. However, the hypothesis is unable to account for the effect of wing sweep, and for any variation of the stress distribution between the lumped flanges otherwise than by estimation of the effective flange area.

It is shown in this paper that in order to account for both sweep and lateral contraction, it is necessary to retain some double products in the stress energy formula: spar direct stress times panel shear, spar direct stress times rib direct stress, etc. Since these terms are omitted when proceeding by the lumping method, the inadequacy of the method is demonstrated. However, the concept of the lumped flange area is very handy and it is used on many occasions in this paper, especially in establishing relationship between the loads, external or redundant internal, and the skin stress components. As far as concerns the stress energy of the wing plate, a continuous stress distribution is assumed so that necessary integrations are always performed over the entire panel, limited by adjacent spars and ribs. In this manner the lumping procedure appears as a mathematical device and not as a physical hypothesis.

In order not to overload the paper with detail the analysis below is limited to the structures shown in figures 1 and 2. The full lines represent shear webs: The spar webs converge to one point and the rib webs are parallel. The structure is symmetric with respect to the middle plane. The upper and lower skin surfaces are planes and have a common trace passing through the intersection point of spar webs. The angle these planes make with the middle plane is very small.

Since with a small number of webs the picture of stress distribution obtained by the lumping method may be

quite crude, fictitious spars and ribs are introduced and represented in the figure by dotted lines. These elements have flanges only, but no shear webs. Their number is arbitrary and is limited by economy reasons only. Lumping of the material into spar flanges real or fictitious, is done as indicated in Fig. 3.

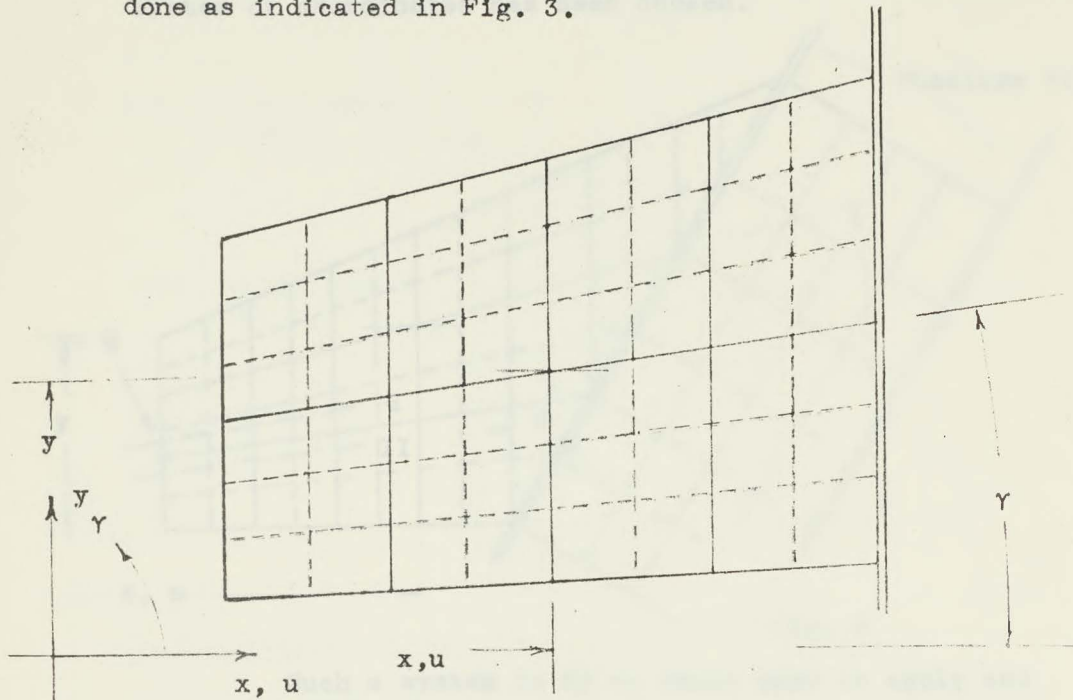


Fig. 1

In this manner the structure is referred to rectangular coordinates x, y and to trapezoidal ones u, γ , between which a transformation holds:

$$x = u, \quad y = u \tan \gamma \quad (1)$$

The directions of the shear webs determine a system of reference for stress components. As a rule, in elasticity systems of reference other than Cartesian are introduced in

order to make the situation at the boundary easier for mathematical work. As, in the present case, forces are fed into panels by shear webs and the panels are of trapezoidal shape, and since no normal stress of any considerable magnitude exists at the leading, or trailing, edge, the trapezoidal system of coordinates has been chosen.

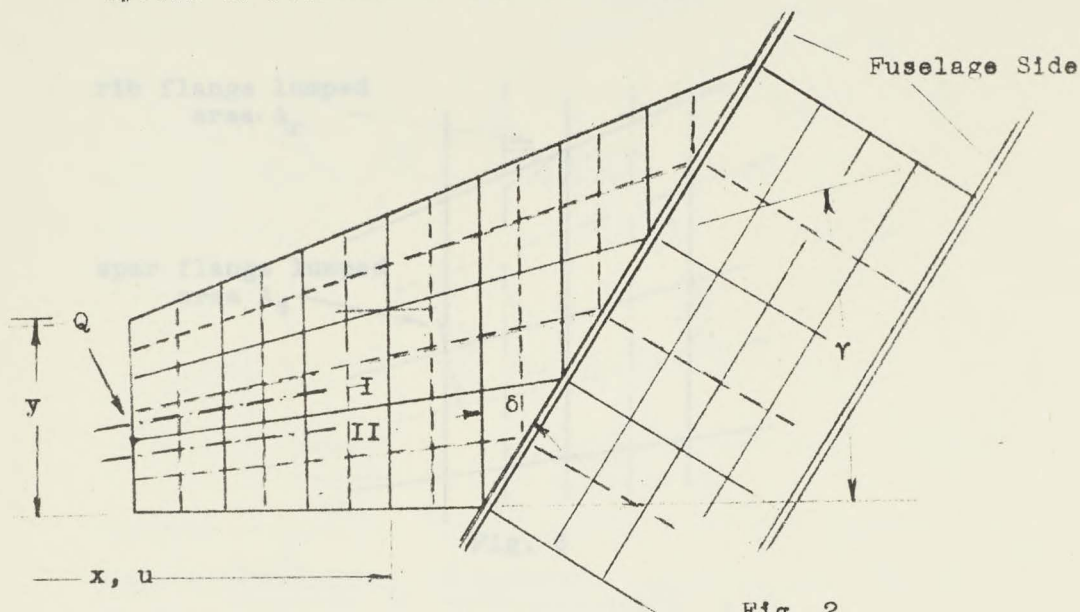


Fig. 2

Such a system is by no means easy to apply and requires some knowledge of the tensor calculus, at least for guidance. In this paper, however, no direct reference to the tensor technique is made and the trapezoidal stress components are eliminated except for the panel shear. However it is necessary to use them at the beginning.

In addition to the main trapezoidal stress components the following are used in the text:

- a) orthogonal stress components σ_x , σ_y , τ_{xy} of the system x, y ,
- b) spar normal stress σ_s ;

c) rib normal stress σ_r .

Stress energy of the panel is expressed in terms of σ_s , σ_r , and of τ_m (average trapezoidal panel shear). Spar, or rib, normal stress is computed by dividing the local bending moment by the lumped area and the local wing plate thickness,

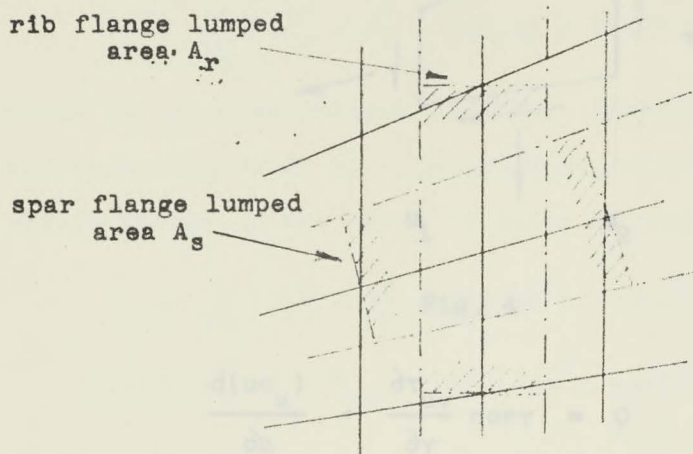


Fig. 3

2. Trapezoidal Stress Components. Energy Formula

Stress components in the trapezoidal system u , γ are denoted by σ_u , σ_γ , $\tau_{u\gamma}$ and defined in fig. 4. In particular with reference to this figure:

$\sigma_u t u_2 (\tan \gamma_2 - \tan \gamma_1)$	means a force in lb. transmitted through the cross section	$t u_2 (\tan \gamma_2 - \tan \gamma_1)$	in the direction of	$\gamma = \text{const.}$
$\tau_{u\gamma} t u_2 (\tan \gamma_2 - \tan \gamma_1)$		$t u_2 (\tan \gamma_2 - \tan \gamma_1)$		$u = \text{const.}$
$\sigma_\gamma t (u_2 - u_1) / \cos \gamma_2$		$t (u_2 - u_1) / \cos \gamma_2$		$u = \text{const.}$
$\tau_{\gamma u} t (u_2 - u_1) / \cos \gamma_2$		$t (u_2 - u_1) / \cos \gamma_2$		$\gamma = \text{const.}$

where t is the skin thickness.

The above stress components satisfy conditions of equilibrium on the infinitesimal element $du.d\gamma$:

$$\tau_{u\gamma} = \tau_{\gamma u}$$

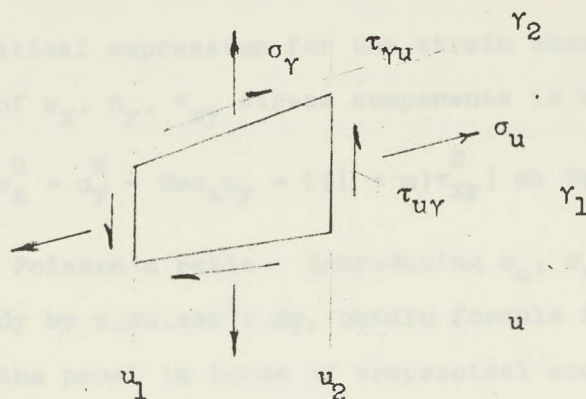


Fig. 4

$$\frac{\partial(u\sigma_u)}{\partial u} + \frac{\partial\tau_{u\gamma}}{\partial \gamma} \cos \gamma = 0$$

$$\frac{\partial(u^2\tau_{\gamma u})}{u\partial u} + \frac{\partial(\sigma_\gamma \sec \gamma)}{\partial \gamma} \cos^2 \gamma = 0$$

(2)

For derivation, see Appendix. By Fig. 5, the following transformation holds between σ_u , σ_γ , $\tau_{u\gamma}$ and σ_x , σ_y , τ_{xy} .

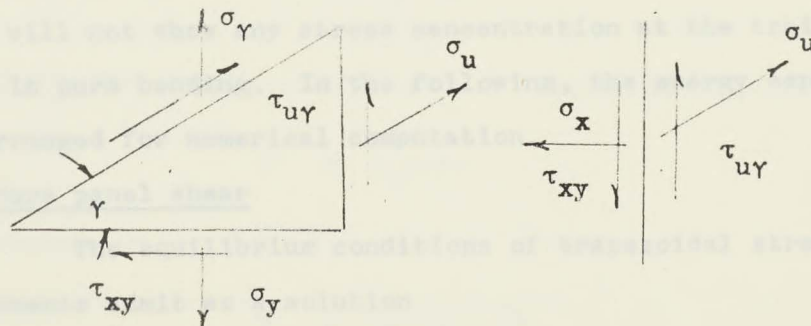


Fig. 5

$$\begin{aligned}\sigma_x &= \sigma_u \cos \gamma \\ \tau_{xy} &= \tau_{uy} + \sigma_u \sin \gamma \\ \sigma_y &= \sigma_\gamma \sec \gamma + 2\tau_{uy} \tan \gamma + \sigma_u \sin \gamma \tan \gamma\end{aligned}\quad (3)$$

A mathematical expression for the strain energy of a sheet in terms of σ_x , σ_y , τ_{xy} stress components is known

$$V = \frac{t}{2E} \int [\sigma_x^2 + \sigma_y^2 - 2m\sigma_x\sigma_y + 2(1+m)\tau_{xy}^2] dx dy$$

where m denotes Poisson's ratio. Introducing σ_u , σ_γ , τ_{uy} and replacing dx, dy by $u, du \cdot \sec^2 \gamma, d\gamma$, obtain formula for the strain energy of the panel in terms of trapezoidal coordinates

$$\begin{aligned}V = \frac{t}{2E} \int & [\sigma_u^2 + \sigma_\gamma^2 - 2(m \cos^2 \gamma - \sin^2 \gamma) \sigma_u \sigma_\gamma + \\ & + 4 \sin \gamma (\sigma_u + \sigma_\gamma) \tau_{uy} + (E/G \cos^2 \gamma + 4 \sin^2 \gamma) \tau_{uy}^2] \frac{u du d\gamma}{\cos^4 \gamma}\end{aligned}\quad (4)$$

Here the particular terms have the following meaning. The τ_{uy}^2 term represents the shear energy of the panel. The σ_u^2 and σ_γ^2 terms are interpreted as bending energy of spars and ribs. The term containing $\sigma_u \sigma_\gamma$ introduces the Poisson's ratio coupling. Finally the term $4 \sin \gamma \tau_{uy} (\sigma_u + \sigma_\gamma)$ takes care of the swept wing coupling; if the term is omitted the computation will not show any stress concentration at the trailing edge in pure bending. In the following, the energy expression is arranged for numerical computation.

a) Pure panel shear

The equilibrium conditions of trapezoidal stress components admit as a solution

$$\sigma_u = 0, \quad \sigma_\gamma = 0, \quad \tau_{uy} = C/u^2 \quad (5)$$

where C is a constant of integration. When transformed into the x, y coordinates the above yields the known distribution

$$\sigma_x = 0, \quad \sigma_y = 2Cy/x^3, \quad \tau_{xy} = C/x^2$$

which evidently does not satisfy the compatibility condition exactly. The solution is used below with this reservation.

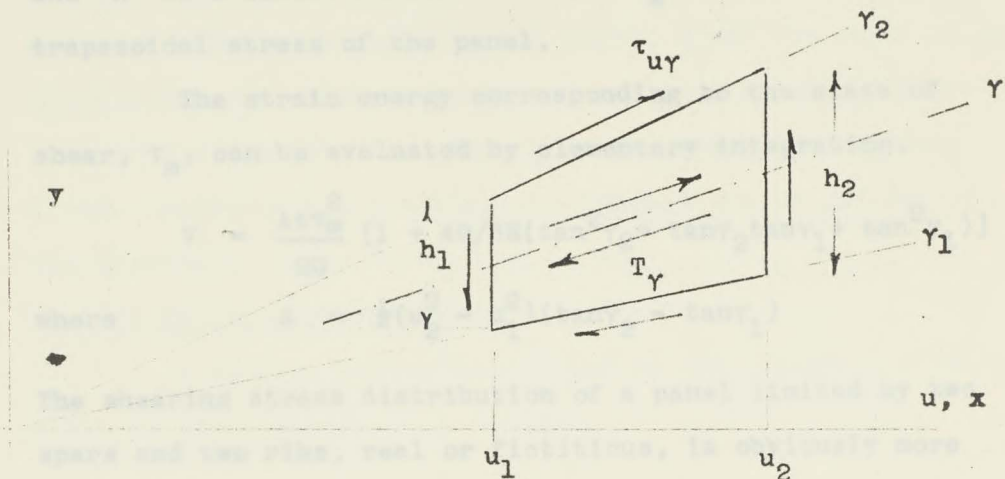


Fig. 6

On any cross section $\gamma = \text{const.}$, the shearing stress gives the resultant

$$T_\gamma = t \int_{u_1}^{u_2} \tau_{u\gamma} du \sec \gamma$$

This force has in the x -direction a component, fig.6,

$$T = T_\gamma \cos \gamma$$

By integration

$$T = tC \frac{u_2 - u_1}{u_2 u_1}$$

Hence the panel shear becomes

$$\tau_{uy} = \tau_m u_1 u_2 / u^2 = \tau_m h_1 h_2 / h^2 \quad (6)$$

where

$$\tau_m = \frac{T}{(u_2 - u_1)t} \quad (7)$$

and h is a linear function of u . τ_m is the average trapezoidal stress of the panel.

The strain energy corresponding to the state of shear, τ_m , can be evaluated by elementary integration.

$$V = \frac{At\tau_m^2}{2G} [1 + 4G/3E(\tan^2\gamma_2 + \tan\gamma_2 \tan\gamma_1 + \tan^2\gamma_1)] \quad (8)$$

where $A = \frac{1}{2}(u_2^2 - u_1^2)(\tan\gamma_2 - \tan\gamma_1)$

The shearing stress distribution of a panel limited by two spars and two ribs, real or fictitious, is obviously more complicated. However, it will be shown later that by using the lumping device it is possible to connect τ_m with the internal redundant loads. Thus, the above formula is a useful approximation of the shear energy of the panel.

b) Spar flange direct stress

According to the lumping method a state of pure tension should be assumed in a spar flange. This state is given by

$$\sigma_{u\sec y} = \sigma_s(s), \quad \sigma_y = 0, \quad \tau_{uy} = 0. \quad (9)$$

$\sigma_s(s)$ is the conventional direct stress of the flange. It varies along the spar due to panel and web shears acting on

the lumped flange. However, it is assumed constant over a certain range of γ , the angular width of the spar flange. Then the strain energy of the flange becomes

$$dV = \frac{1}{2E} \sigma_s^2(s) A_s(s) ds \quad (10)$$

A_s is the spar flange lumped area and s is the length coordinate, and $ds = du \sec \gamma$. On the assumption that panels and webs develop shearing stress only, $\sigma_s(s)$ for each flange segment depends on the values of the flange stress at both ends of the segment, i.e. on σ_s at two spar/rib intersections. Since $A_s(s)$ is known the formula can be integrated. See Appendix.

c) Rib flange direct stress

A similar reasoning applied to rib flanges yields a state of pure tension in a flange

$$\sigma_u = 0, \quad \sigma_{\gamma \sec \gamma} = \sigma_r(r), \quad \tau_{u\gamma} = 0. \quad (11)$$

and expression for the strain energy of the rib flange becomes

$$dV = \frac{1}{2E} \sigma_r^2(r) A_r dr \quad (12)$$

A_r is the rib flange lumped area and r is the length coordinate, and $dr = dy$.

As before $\sigma_r(r)$ depends on the values the flange stress attains at two spar/rib intersections at both ends of the rib flange segment.

d) Coupling terms

It is understood here that for large angles of sweep the rib arrangement indicated in figure 2 would be adopted

in preference to the arrangement of figure 1. Therefore γ is not a very large angle and the sweep coupling term is rather a correction. On introducing spar and rib direct stresses, the integrands of the coupling terms become:

i) Poisson's ratio

$$(m \cos^2 \gamma - \sin^2 \gamma) \sigma_r \sigma_s = [\sigma^2]$$

ii) panel sweep

$$\tan \gamma \tau_{uy} (\sigma_r + \sigma_s) = [\sigma \tau]$$

Remembering $dA = u \, du \, dy \sec^2 \gamma$ and taking some weighted averages of the values σ_r , σ_s defined in the four corners of the panel and introducing the average trapezoidal shearing stress τ_m in the latter expression, the integrals become

$$i) \quad V = \frac{-At}{E} [\sigma^2]_{av} \quad (13)$$

$$ii) \quad V = \frac{2At}{E} [\sigma \tau]_{av} \quad (14)$$

Thus strain energy of the structure can be written in terms of σ_s and σ_r known at each spar/rib intersection and of τ_m for each trapezoidal panel. The formulae are exact in the limit $A \rightarrow 0$. See Appendix.

3. Redundant Moments of the First Kind

Let Q be a unit load acting perpendicularly to the wing plate of figure 2. The statically determinate part of stress distribution due to Q is obtained by severing the structure along the lines I and II, and amounts to a simple spar bending. Were it expedient, sometimes, to introduce a torque as a unit load, the statically

determinate stress would be the simple Batho shear flow around the whole wing cross section or a part of it. Of course, any stress distribution obtained in this manner does not meet the condition of compatibility of strains and should be corrected by redundant distributions satisfying the theorem of least work.

Consider a wing plate as represented in figures 1 and 2, with the difference that the whole skin material is lumped over the existing real webs i.e. all intermediate spars and ribs have been omitted. Suppose that the structure is subdivided in separate cells by cuts made through the internal webs, and assume for simplicity: -

- a) all webs are infinitely stiff in shear, however, they do not oppose any extension or compression of flanges;
- b) no strain exists in webs in the direction perpendicular to the middle plane of the wing; and further
- c) flange extension does not affect the shearing stress of adjacent panels.

Since material lumping is a mathematical device only, the latter statement expresses merely the principle of superposition of stress components.

- Incompatibility of deformation due to some assumed statically possible stress system can be visualized thus: Suppose all cells have been manufactured to the dimensions they would acquire under the assumed stress if they were isolated and free to deform. In general it would not be possible to fit the structure together without gaps, and

any isolated cells could always be fitted in three corners of their common wall, but not in all four corners. In other words cells would behave as a four legged table on an uneven floor. This suggests the following concept of statically indeterminate groups of stress.

Assume, by hypothesis, that the redundant interaction of any two adjacent cells is reduced to a group of four forces applied perpendicularly to, and in four corners, of the common face or wall. See figure 7. Forces acting on adjacent cells are opposite to those drawn in the figure. Forces of

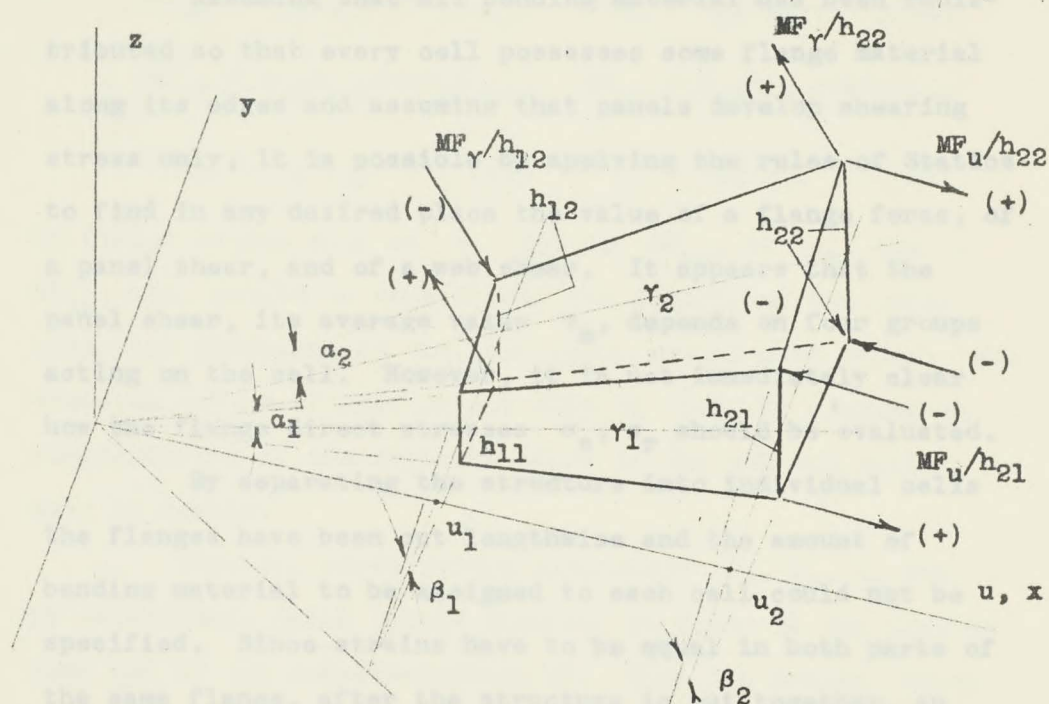


Fig. 7

one group are expressed in terms of a bimoment quantity MF as shown in the figure. In particular, bimoments or warping groups MF_u act on or through faces $u = \text{const.}$, bimoments or warping groups MF_γ act on or through faces $\gamma = \text{const.}$ By hypothesis, each group produces stresses in elements of two wing cells only. Thus all isolated cells are considered as statically determinate as it concerns their loading by redundant groups. Incomplete cells, with a side web missing for instance, are statically impossible and structures of that kind are not the object of this paper.

Assuming that all bending material has been redistributed so that every cell possesses some flange material along its edges and assuming that panels develop shearing stress only, it is possible by applying the rules of Statics to find in any desired place the value of a flange force, of a panel shear, and of a web shear. It appears that the panel shear, its average value τ_m , depends on four groups acting on the cell. However, it is not immediately clear how the flange direct stresses σ_s, σ_r should be evaluated.

By separating the structure into individual cells the flanges have been cut lengthwise and the amount of bending material to be assigned to each cell could not be specified. Since strains have to be equal in both parts of the same flange, after the structure is put together, an additional redundancy must exist so as to provide for a proper redistribution of the flange forces. Consequently σ_s, σ_r are equal to the difference of two flange forces, as

computed from adjacent cells, divided by the total lumped cross section of the flange, and the additional redundancy does not have to be considered.

Denoting:

$$b_1 = u_1(\tan \gamma_2 - \tan \gamma_1), \quad b_2 = u_2(\tan \gamma_2 - \tan \gamma_1), \quad a = u_2 - u_1;$$

$$a_1 = a \sec \gamma_1, \quad a_2 = a \sec \gamma_2 \quad \text{one obtains, see Appendix,}$$

$$MF_{u2}b_1 - MF_{u1}b_2 + MF_{\gamma2}a_2 - MF_{\gamma1}a_1 = a(h_{11}b_2 + h_{22}b)t \cdot \tau_m \quad (15)$$

$$MF_{u1} = h_{12}A_{s12} \cos \gamma_2 \sigma_{s12}, \quad MF_{u2} = h_{22}A_{s22} \cos \gamma_2 \sigma_{s22} \quad (16)$$

$$-MF_{u1} = h_{11}A_{s11} \cos \gamma_1 \sigma_{s11}, \quad -MF_{u2} = h_{21}A_{s21} \cos \gamma_2 \sigma_{s21}$$

$$-MF_{\gamma2} = h_{12}A_{r12} \cos \gamma_2 \sigma_{r12}, \quad MF_{\gamma2} = h_{22}A_{r22} \cos \gamma_2 \sigma_{r22} \quad (17)$$

$$-MF_{\gamma1} = h_{11}A_{r11} \cos \gamma_1 \sigma_{r11}, \quad MF_{\gamma1} = h_{21}A_{r21} \cos \gamma_1 \sigma_{r21}$$

No flange stress such as σ_r due to MF_{u2} , or σ_s due to $MF_{\gamma2}$, etc. should be considered, the effects of two cells under the influence of the same group cancel each other. The shearing stress of spar or rib webs is found by summing up contributions of two adjacent cells on the web the cells have in common.

Thus all three stress components σ_r , σ_s , τ_m can be established (with little trouble) in terms of the applied load and of the redundant groups MF . Then the stress components are substituted in the energy formula and the second theorem of Castigliano is applied. Hence all group values MF are obtained by solving a set of linear equations. It is

discussed later how this somewhat enormous operation should be performed. There can be no question, that, as long as the number of unknowns is small, the procedure should not present any difficulties from the mathematical point of view. What is debatable is the accuracy of the solution obtained which, probably, should not be large for a two or three spar structure. The main question is whether the whole procedure makes any sense at all with a large number of spars and ribs. The answer to this important question is in the affirmative, and we proceed to show that in the case of a rectangular grid of webs, with the web spacing approaching zero, the above group functions MF_u and MF_v become the Southwell stress functions of the plate theory.

PROOF

Assume a rectangular grid of webs as indicated in Fig. 8.

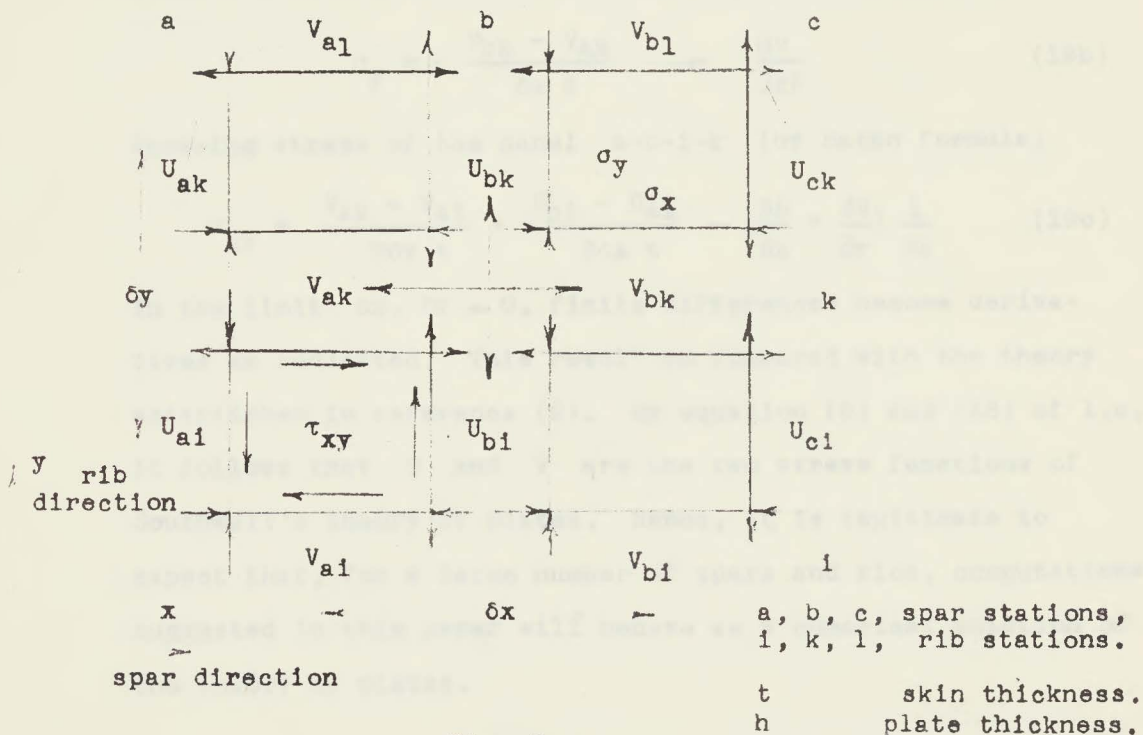


Fig. 8

Ribs may be spaced by δx and spars by δy . The plate thickness h may be constant all over the wing. Hence the four forces belong to one redundant group are of the same magnitude. Denote group forces acting in the x direction by U and group forces acting in the y direction by V . Then in notations of the figure ($dy = u \, d\gamma$).

$$U = MF_x/h, \quad V = MF_y/h \quad (18)$$

Both U and V vary from one face to another. Spar, rib, and panel stress due to group forces is given as follows:

Bending stress of the spar k at the rib b

$$\sigma_x = - \frac{U_{bk} - U_{bi}}{\delta y \, t} \rightarrow \frac{\partial U}{\partial y t} \quad (19a)$$

Bending stress of the rib b at the spar k

$$\sigma_y = - \frac{V_{bk} - V_{ak}}{\delta x \, t} \rightarrow \frac{\partial V}{\partial x t} \quad (19b)$$

Shearing stress of the panel $a-b-i-k$ (by Batho formula)

$$\tau_{xy} = \frac{V_{ak} - V_{ai}}{2\delta y \, t} + \frac{U_{bi} - U_{ai}}{2\delta x \, t} \rightarrow \left[\frac{\partial U}{\partial x} + \frac{\partial V}{\partial y} \right] \frac{1}{2t} \quad (19c)$$

In the limit $\delta x, \delta y \rightarrow 0$, finite differences become derivatives as indicated. This result is compared with the theory established in reference (2). By equation (8) and (36) of l.c., it follows that U and V are the two stress functions of Southwell's theory of plates. Hence, it is legitimate to expect that, for a large number of spars and ribs, computations suggested in this paper will behave as a numerical solution of the theory of plates.

4. Redundant Moments of the Second Kind

If there are only few spars on the chord line, the shear lag effect between spars becomes appreciable, and the accuracy of a stress distribution obtained by methods of Para.3 may be in doubt. The solution can be improved, however by introducing another redundant quantity MF . While the MF groups were related to the Southwell stress functions, the new quantity is akin to the Airy Function.

Consider, with reference to figure 8, a quadruple cell extending from u_1 to u_3 and from γ_1 to γ_3 with intermediate webs at u_2 and γ_2 . By severing the structure through the middle plane and taking moments around the web intersection line at u_2, γ_2 one can show easily that no shearing stress is assigned to all external webs if the relations hold:

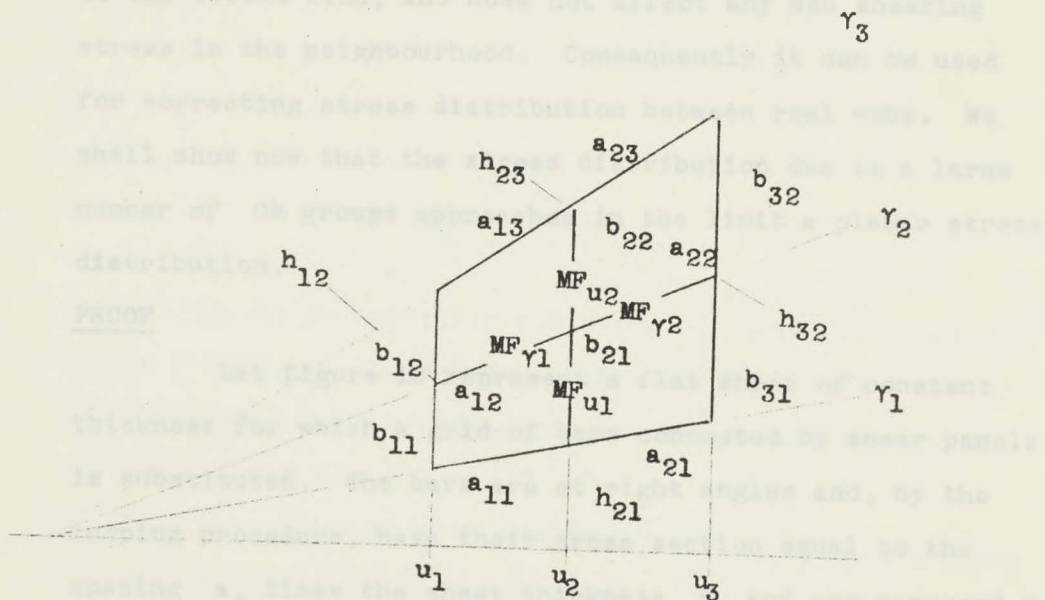


Fig. 9

$$\begin{aligned} \frac{MF_{u2}b_{22}}{h_{23}} + \frac{MF_{\gamma 1}a_{12}}{h_{12}} &= -\frac{MF_{u2}b_{22}}{h_{23}} + \frac{MF_{\gamma 2}a_{22}}{h_{32}} = 0 \\ -\frac{MF_{u1}b_{21}}{h_{21}} + \frac{MF_{\gamma 1}a_{12}}{h_{12}} &= \frac{MF_{u1}b_{21}}{h_{21}} + \frac{MF_{\gamma 2}a_{22}}{h_{32}} = 0 \end{aligned}$$

But then, there is no shearing stress in the internal webs either, as follows from the equilibrium condition of the common edge of three webs a_{13} , a_{23} , b_{22} .

The above four groups MF can be derived from a single quantity MG such that

$$\begin{aligned} MF_{u1} &= MG h_{21}/b_{21}, & MF_{u2} &= -MG h_{23}/b_{22}, \\ MF_{\gamma 1} &= MG h_{12}/a_{12}, & MF_{\gamma 2} &= -MG h_{32}/a_{22}, \end{aligned} \quad (20)$$

By definition the trimoment MG is the redundant quantity of the second kind, and does not affect any web shearing stress in the neighbourhood. Consequently it can be used for correcting stress distribution between real webs. We shall show now that the stress distribution due to a large number of GM groups approaches in the limit a planar stress distribution.

PROOF

Let figure 10 represent a flat sheet of constant thickness for which a grid of bars connected by shear panels is substituted. The bars are at right angles and, by the lumping procedure, have their cross section equal to the spacing a , times the sheet thickness t , and are supposed to develop direct stress only. The connecting shear panels

carry shearing stress only.

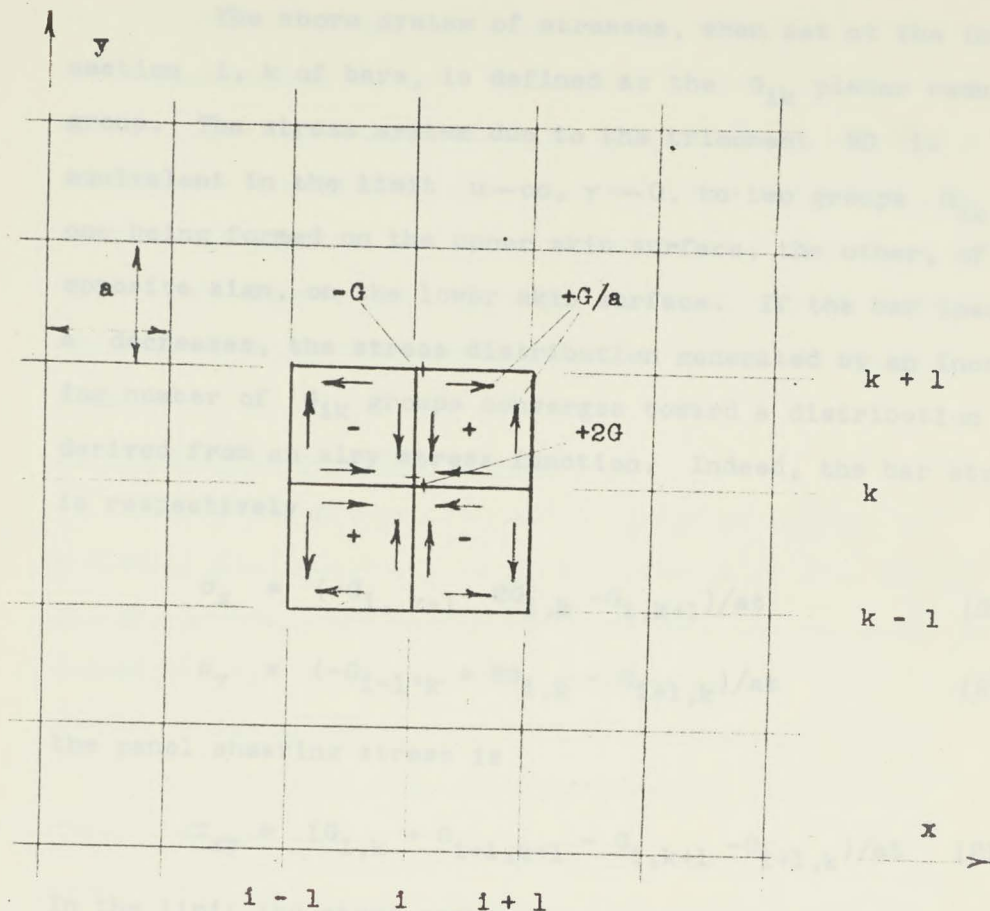


Fig. 10

By cutting out an assembly consisting of three bars parallel to the x-axis, of three bars parallel to the y-axis, and of four panels, a self equilibrated system of stresses can be defined. There are

- 1) four panel shears of the magnitude $\pm G/a$ lb/in
- 2) at the centre the bars are in tension equal to $2G$ lb
- 3) at mid points of four sides the bars are in compression $- G$ lb

- 4) no bar stress exists at the four corners of the assembly.

The above system of stresses, when set at the intersection i, k of bars, is defined as the G_{ik} planar redundant group. The stress system due to the trimoment MG is equivalent in the limit $u \rightarrow \infty, \gamma \rightarrow 0$, to two groups G_{ik} , one being formed on the upper skin surface, the other, of opposite sign, on the lower skin surface. If the bar spacing a decreases, the stress distribution generated by an increasing number of G_{ik} groups converges toward a distribution derived from an Airy stress function. Indeed, the bar stress is respectively,

$$\sigma_x = (-G_{i, k-1} + 2G_{i, k} - G_{i, k+1})/at \quad (21a)$$

$$\sigma_y = (-G_{i-1, k} + 2G_{i, k} - G_{i+1, k})/at \quad (21b)$$

the panel shearing stress is

$$\tau_{xy} = (G_{i, k} + G_{i+1, k+1} - G_{i, k+1} - G_{i+1, k})/at \quad (21c)$$

In the limit the above expressions become

$$\sigma_x t/a = -\frac{\partial^2 G}{\partial y^2}, \quad \sigma_y t/a = -\frac{\partial^2 G}{\partial x^2}, \quad \tau_{xy} t/a = \frac{\partial^2 G}{\partial x \partial y} \quad (22)$$

Thus G_{ik} can be used as a stress function with a method proceeding with finite differences. Hence, any system of G_{ik} satisfying the second theorem of Castigliano, for some assumed statically determinate stress distribution, is an approximate solution of a planar stress problem.

The groups G_{ik} are the only ones which can be

used in plane stress problems. In plate problems, however, the groups, or rather their associated trimoments $MG = Gh$, are complementary to the MF warping groups introduced in para.3. One can expect that the relationships proved for rectangular coordinates and constant plate thickness will hold for trapezoidal coordinates and tapered plates as well. Thus a way appears open for numerical analysis of swept and tapered wing plates with practically any arrangement of webs.

5. Analysis by Redundant Groups

If MG groups are used in order to improve an analysis, which would not be satisfactory when done solely by MF groups, care should be taken that not too many MG groups are put in operation. For instance, no MG group should be placed where four real webs intersect.

Consider a wing plate as shown in figure 11, clamped at the root.

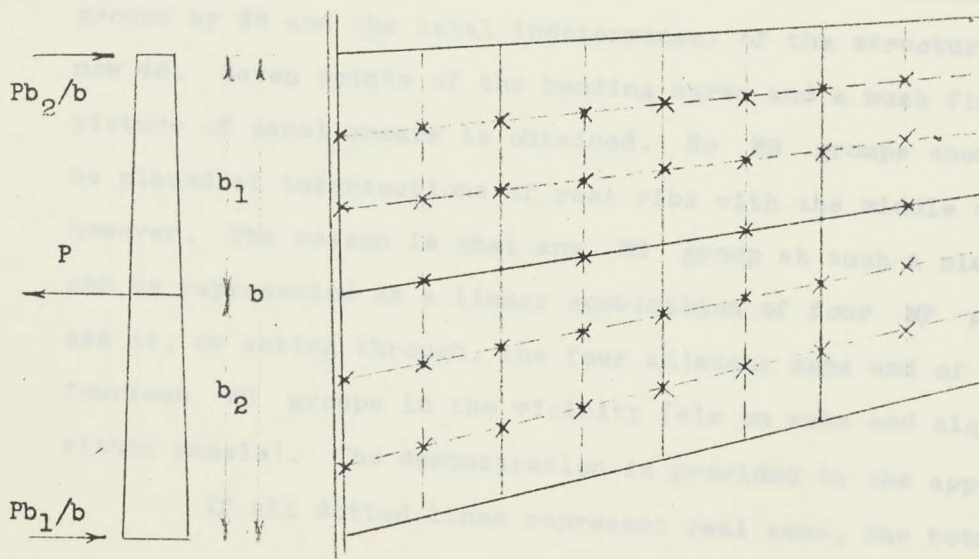


Fig. 11

The full lines may denote real webs and the dotted ones fictitious webs. Suppose at first that all bending material is lumped along the real webs. Thus a redundant group is set on each web common to two cells, and two groups at the boundary. This gives 12 groups of the type MF. The statically determinate part of the stress distribution is simple beam bending. An analysis of this kind has been made for a four beam structure and results are shown further below. As far as concerns the case of figure 11 it is quite obvious that the accuracy of a computation with 12 redundancies may not be satisfactory since only three points of the bending stress curve are obtained at each cross section. Similarly, the information on panel shearing stress is very poor and reduces to two values at the root.

A better approximation is reached if MG groups are introduced in all points marked by x, and lumping is changed accordingly. This increases the number of redundant groups by 36 and the total indeterminacy of the structure is now 48. Seven points of the bending curve and a much finer picture of panel shears is obtained. No MG groups should be placed at intersections of real ribs with the middle spar, however. The reason is that any MG group at such a place can be represented as a linear combination of four MF groups set at, or acting through, the four adjacent webs and of fourteen MG groups in the vicinity (six on webs and eight within panels). The demonstration is provided in the appendix.

If all dotted lines represent real webs, the total

redundancy of the structure is increased to 88. An additional redundancy may appear at the clamped boundary if some vertical displacement of the foundation is possible. Two cases should be considered:

- a) No displacement is possible at the root. In this event all elements of the root rib are assumed infinitely rigid, and the derivatives of the stress energy function are put equal to zero as indicated by the Castigliano theorem.
- b) The root is not rigid and some vertical displacement of the foundation can occur but no rotation of the spar ends. In this case a third type of self equilibrated groups, referred to as group P or MP , has to be introduced and terms incorporating the foundation energy added to the total energy of the system. The group P is composed of three forces, acting perpendicularly to the plate as shown in figure 11. Then a condition, $\frac{\partial V}{\partial P} = 0$, expresses that displacement of the point of application of one group force relatively to the points of application of the other two forces is the same for both the wing plate and the foundation. In general the number of groups P at the foundation is equal to the number of spars less two. It is understood that forces composing a group P are in reality not concentrated but represent a distributed action. Here again the principle of lumping is used to advantage in simplifying the computation.

The boundary condition of figure 2 is discussed in the next section.

6, Oblique Boundary Condition

This condition is a topic in itself. In order to generalize, let us assume that the structure consists, see Fig. 12, of a swept outboard part, and of a straight inboard part. The first rib of the unswept part is referred to, subsequently, as the rib at the oblique boundary, as the common rib, or simply as the rib "R".

The main difficulty encountered with this problem can be summed up in the following manner: Since the system of coordinates of a multi spar/rib structure is prescribed by the direction of spars and ribs, both stress and displacement on either side of the oblique boundary are related to different coordinates. Hence the necessity, when establishing conditions of equilibrium at this boundary, to perform a transformation of stress components. The lumping method used in this paper assumes, however, that the skin between spars carries shearing stress only. This assertion cannot be transferred to the other system, for it is known that the state of stress denoted as pure shear exhibits normal stress on any oblique cross section. Thus the lumping method, which merely results in inaccuracy, if the computation remains in one system of coordinates, amounts to a contradiction when a transformation is involved. It follows that the distribution of stress components at the oblique boundary cannot be transformed in the ordinary way and that the device of lumping must be incorporated somehow in the transformation procedure.

This method has already been used by other authors. In the extension of the procedure it is assumed that the triangular cells of the outboard part are protruding inboard so as to form full quadrilateral boxes, to any one of which four redundant groups can be applied. Thus two purposes are served: First, a sufficient number of parameters is provided so that stress of any spar or rib at the boundary can be altered as, and if, required by the condition of minimum strain energy. Hence in the example of Fig. 12 all sixteen stress values, denoted \times , are uniquely determined by one statically determined system and by 15 indeterminate groups.

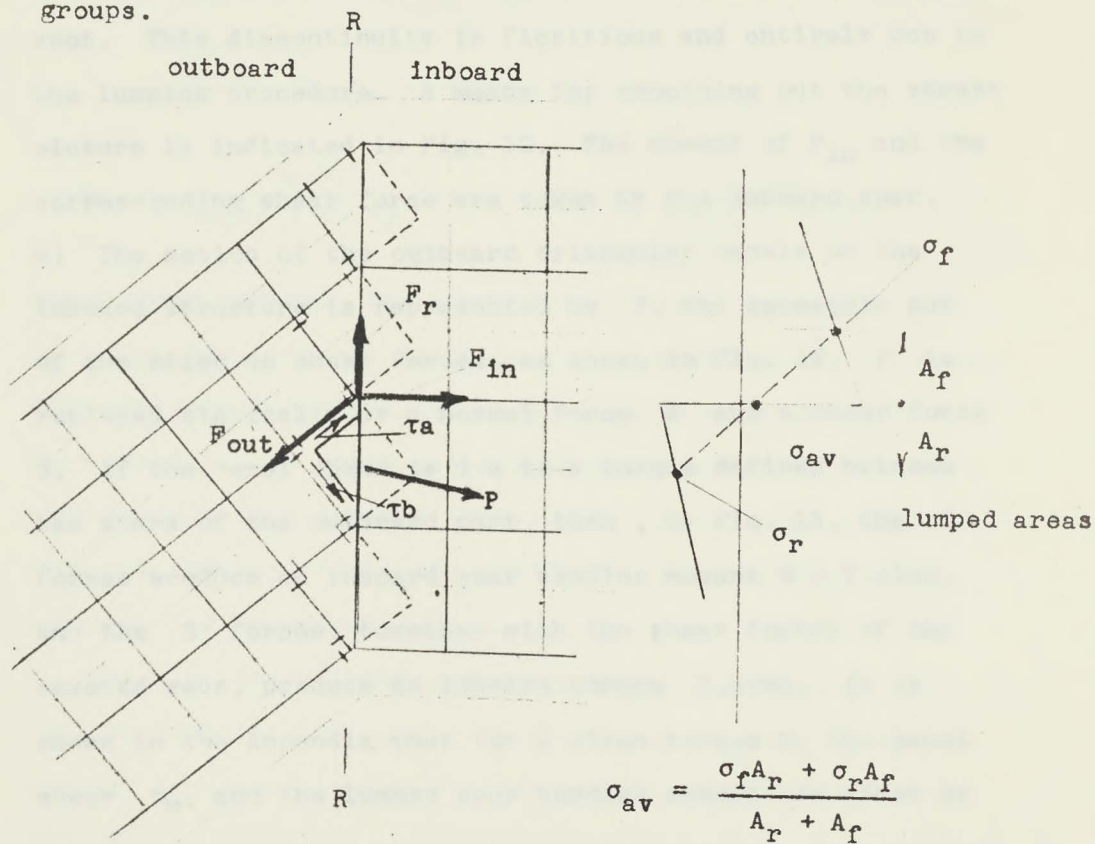


Fig. 12

Secondly, shearing stress need not be assumed to be zero in all triangular cells adjacent to the boundary, as it would appear if the lumping method were followed strictly. Then the structure is severed along the line R - R and the action of the outboard part on the inboard part is considered.

a) Any spar or rib flange force, generated in the outboard part and applied to the inboard one, is resolved in two components, parallel to the direction of the inboard flanges, and parallel to the flange of "R". See Fig. 12, vectors F_{out} , F_{in} , F_r . Since the moment produced by F_r is reacted by the shear flow of the inboard torque box, evidently a discontinuity of the flange stress of "R" is present at this spot. This discontinuity is fictitious and entirely due to the lumping procedure. A means for smoothing out the stress picture is indicated in Fig. 12. The moment of F_{in} and the corresponding shear force are taken by the inboard spar.

b) The action of the outboard triangular panels on the inboard structure is represented by P , the geometric sum of the piled up shear forces, as shown in Fig. 12. P is replaced statically by a normal force N and a shear force S . If the panel shear is due to a torque defined between two spars of the outboard part, then, by Fig. 13, the N forces produce an inboard spar bending moment $M = T \cdot \sin \alpha$, and the S forces, together with the shear forces of the severed webs, produce an inboard torque $T \cdot \cos \alpha$. It is shown in the Appendix that for a given torque T , the panel shear τ_m , and the lumped spar bending moment are given by

three groups of stress:

First group consists, Fig. 15, of the normal to "R" components of the flange forces and of the lumped panel action N. The group generates a warping bimoment MH applied to the inboard part at the rib "R".

Second group is made of a part of the panel action S together with the web shears τ_w of the cut spars or ribs outboard. This is a self equilibrated system which is absorbed by the shear web of "R" at this place. Since all webs are assumed stiff in shear this group does not penetrate any further inboard.

Third group consists, Fig. 16, of the chordwise components of the flange forces and of what is left of the panel action S. This is also a self-equilibrated system which does penetrate inboard, however.

In order to see what the last action amounts to, consider the warping groups MF_y to be set on the spars of the inboard part. See Fig. 16. Since the chordwise stress generated by these groups is a difference of two group values (divided by the rib flange area of course), the same must be true of the flange stress of "R". One should expect, therefore, that a combination of the redundant quantities of the outboard part affects the stress of this flange. Moreover, if no such action were present the stress systems of both parts of the structure would not influence one another except by the MH groups. The necessary additional link is provided by the third stress group as it appears clearly from Fig. 16.

Suppose that $MF_{\gamma 21} = MF_{\gamma 22}$ and that all other groups are zero. In this case no stress exists in the rib flange acted upon by two non zero groups. However, the two S forces remain and produce, in the case of the figure, a local extension of the "R" flange denoted (+). Apparently, the effect is similar to the action of a force of any group MF_y shown in the figure. The resulting strain depends on the full group value, (not on a difference of two group values), and is toned down subsequently by the neighbour group MF_y .

In the general case all warping groups have different values. Thus the above action is conceived as a function of a whole set of warping groups affecting this particular grid point of "R". In the following the action is referred to as the redundant rib moment MR . It is shown in the Appendix that for cells having "R" as a diagonal the warping moment MH has the value:

$$\begin{aligned} MH_1 = & \frac{MF_{u21}}{\cos \gamma_2} m_1 \cos(\alpha + \gamma_2) + \frac{MF_{u11}}{\cos \gamma_1} m_2 \cos(\alpha + \gamma_1) \\ & + \frac{MF_{\gamma 21}}{\cos \gamma_2} m_1 \sin \alpha + \frac{MF_{\gamma 11}}{\cos \gamma_1} m_2 \sin \alpha \end{aligned} \quad (25)$$

Then for grid points on "R"

$$\begin{aligned} MR_2 = & - (MF_{u21} n_2 + MF_{u22} n_1) \frac{\sin(\alpha + \gamma_2)}{\cos \gamma_2} \\ & + (MF_{\gamma 21} n_2 + MF_{\gamma 22} n_1) \frac{\cos \alpha}{\cos \gamma_2} \end{aligned} \quad (26)$$

In the above

$$m_1 = \frac{h_{11} b_2}{h_{11} b_2 + h_{22} b_1} \quad n_1 = \frac{A_r}{A_f + A_r}$$

$$m_2 = 1 - m_1 \quad n_2 = 1 - n_1$$

are the weight factors.

See Figs. 12 and 16 for definition of lumped areas. Similar formulae can be established for other cells and grid points of "R", by conveniently raising the indices in conformity with Fig. 16.

(25) and (26) are the transformation equations of redundant quantities. In order to grasp their true meaning, suppose, for simplicity, that the part outboard of "R" is of constant plate thickness with ribs and spars at right angles. The new system of reference is written u, v , instead of u, γ , with v as a length coordinate. Dividing by h the equations become:

$$H = (F_{u21} + F_{u11}) \frac{\cos \alpha}{2} + (F_{v21} + F_{v11}) \frac{\sin \alpha}{2}$$

$$R = -(F_{u21} + F_{u22}) \frac{\sin \alpha}{2} + (F_{v21} + F_{v22}) \frac{\cos \alpha}{2}$$

and, further with the grid getting smaller and smaller:

$$H = F_u \cos \alpha + F_v \sin \alpha$$

$$R = -F_u \sin \alpha + F_v \cos \alpha$$

One sees that the forces composing the warping groups of the first kind transform as vectors when passing from one system of reference to the other. This should be expected. By (19) of Chapter II, 3, H, R, F_u, F_v are the Southwell stress functions of the plate theory and their law of transformation should be compatible with the law of transformation of stress components. It can be shown, after some work, by direct substitution that the stress components will transform by

the known formulae, when passing from one system to the other, only if the Southwell's stress functions transform as indicated above.

III, NUMERICAL OPERATIONS

1. Matrix Notation

It is apparent from the preceding analysis that the numerical work, for any structure of practical significance, is quite extensive. A good digital computer is required in order to digest the quantity of data. However, the preparation of data for the computer is a difficult task, since all material fed into the computer must be error free and since the automatic process, when once started, has to be carried out to the end. Therefore all preparation of data, their checking, and presentation must be done as neatly and orderly as possible. The indispensable mathematical tool which makes the whole work feasible is the matrix calculus and technique. At this place, a few particulars of the adopted notation are explained as there are differences, and preferences, among different authors.

In this paper matrices are denoted by letters, mostly capital ones, with appended indices as for instance S_{ia} , Z_{ab} , F_p . Three groups of indices are introduced:

1) Load point indices

$$a, b, c = 1, 2, 3, \dots$$

to indicate position where a load is applied or where deflection is measured. A symbol, such as Q_a denotes a load applied to the structure, and z_a denotes a deflection at the load

point a.

2) Stress section indices

$$i, k, l = 1, 2, 3, \dots$$

indicate cross sections or spots where stress is, or is proposed to be, determined. Thus S_i denotes all stress values such as $\sigma_s, \sigma_r, \tau_m$ at spar rib intersections, or at panels. In particular \bar{S}_i denotes the statically determinate part of the stress distribution.

3) Redundant group indices

$$p, q, r = 1, 2, 3, \dots$$

Thus F_p denotes any redundant quantity or group.

Indices are interchangeable within each group, e.i.

1 can always be written for k and k for i. However, one is not allowed to use, say a p letter in order to denote a load point. Q_a, S_i , and F_p are vectors in the matrix language. From the point of view of mechanical computation the distinction between a column and a row vector is immaterial, since each one is represented by a similar deck of punched cards or by a similar sequence of marks on a tape.

At any cross section i stress is a linear function of an applied load and of a redundant load. This relationship is written in the adopted notation

$$S_i = T_{ia} Q_a + K_{ip} F_p \quad (27)$$

where T_{ia} is the statically determinate stress-to-load matrix and K_{ip} is the stress-to-redundant-load matrix. A convention is borrowed from the tensor calculus: a repeti-

tion of an index means that a summation is carried out through all index values. A repeated index can be designated by any letter of the same group provided the letter has not been used in the same term already. Interchanging indices of different groups, e.i. writing T_{ai} for T_{ia} , would conventionally mean that a matrix is being transposed.*) However, from the point of view of mechanical computation, again it is immaterial how a matrix is written. What matters is how the matrix is marked on a tape or how the punched cards are shuffled. So for instance a matrix A_{pi} where $i = 1, 2, 3, 4, 5$, $p = 1, 2, 3$, e.i. an array

1	—
p	x x x x x
x	x x x x x
x	x x x x x

can be marked on the tape or shuffled by the p index in the sequence

$p =$	1	2	3
	x x x x x	x x x x x	x x x x x
$i =$	1 2 3 4 5	1 2 3 4 5	1 2 3 4 5

or by the i index in the sequence

$i =$	1	2	3	4	5
	x x x	x x x	x x x	x x x	x x x
$p =$	1 2 3	1 2 3	1 2 3	1 2 3	1 2 3

which of two arrangements is used depends on whether the matrix is a post or a premultiplier. So for instance in a multiplication represented symbolically by

*) See p.42.

$$A_{ai} B_{ip} = C_{ap}$$

or graphically by

$$\begin{array}{c}
 \begin{array}{c} i \longrightarrow \\ a \downarrow \end{array} \begin{array}{|c|c|c|c|} \hline x & x & x & \\ \hline x & x & x & \\ \hline x & x & x & \\ \hline x & x & x & \\ \hline x & x & x & \\ \hline \end{array} \cdot \begin{array}{c} \begin{array}{c} p \longrightarrow \\ 1 \downarrow \end{array} \begin{array}{|c|c|c|c|c|} \hline x & x & x & x & x \\ \hline x & x & x & x & x \\ \hline x & x & x & x & x \\ \hline \end{array} \\
 \end{array} = \begin{array}{c} \begin{array}{c} p \longrightarrow \\ a \downarrow \end{array} \begin{array}{|c|c|c|c|c|} \hline x & x & x & x & x \\ \hline x & x & x & x & x \\ \hline x & x & x & x & x \\ \hline x & x & x & x & x \\ \hline x & x & x & x & x \\ \hline \end{array}
 \end{array}$$

the premultiplier is arranged by a row index a , and the postmultiplier by a column index p . It is entirely up to the operator how the product will emerge from the machine and his judgment will depend on how he intends to use the result, as a post- or a premultiplier, in further work. The rule is as follows: in any simple matrix multiplication such as $A_{ai}B_{ip}$ the matrices have to be arranged by indices which are not summation indices. For these reasons it is not important for this work whether a distinction is made between an original and a transposed position of a matrix. It is important, however, that any established formula presents a clear program of operation to the computer.

Strain energy is computed at first for each particular element such as a flange, a panel, in terms of stress components, then a summation is carried out for the whole structure. In the result

$$V = \frac{1}{2} C_{ik} S_i S_k$$

where C_{ik} is a symmetric square matrix of order i . The above notation is satisfactory for paper work, of course. It does not indicate the sequence of operations, however. The

required notation is

$$V = \frac{1}{2} S_i C_{ik} S_k \quad (28)$$

and is used as a starting expression in the work below.

2. Stress to load matrix S_{ia}

In the notation of the last section, the stress at any significant cross section is a sum of the statically determinate part $S_i^0 = T_{ia} Q_a$ and the redundant part: thus

$$S_i = S_i^0 + K_{ip} F_p \quad (29)$$

On substitution in the energy expression, we obtain:

$$V = \frac{1}{2} (F_p K_{pi} + S_i^0) C_{ik} (S_k + K_{kq} F_q)$$

Here, in the second term on the right hand a new index q has to be introduced according to the rules of operating with summation indices.

When carrying out the indicated multiplications one has to consider that the two products, as marked above, are equal. Hence the energy formula becomes

$$V = \frac{1}{2} S_i^0 C_{ik} S_k^0 + F_p K_{pi} C_{ik} S_k^0 + \frac{1}{2} F_p K_{pi} C_{ik} K_{kq} F_q \quad (30)$$

With the notation

$$K_{pi} C_{ik} = H_{pk}, \quad K_{pi} C_{ik} K_{kq} = D_{pq}$$

the energy formula is written

$$V = \bar{V} + F_p H_{pk} S_k^0 + \frac{1}{2} F_p D_{pq} F_q$$

$\overset{0}{V}$ is the statically determinate portion of strain energy, not required at the present time. D_{pq} is a symmetric matrix. By the second theorem of Castigliano

$$\partial V / \partial F_q = H_{qk} \overset{0}{S}_k + F_p D_{pq} = 0 \quad (31)$$

Here the index q denotes the equation and the index p the unknown in the equation. Let D_{pq}^{-1} be a matrix inverse to D_{pq} . Then the solution of the above set is given by

$$F_p = -D_{pq}^{-1} H_{qk} \overset{0}{S}_k \quad (32)$$

Thus

$$S_i = \overset{0}{S}_i - K_{ip} D_{pq}^{-1} H_{qk} \overset{0}{S}_k$$

or, introducing the Kronecker delta δ_{ik} ,

$$S_i = (\delta_{ik} - K_{ip} D_{pq}^{-1} H_{qk}) \overset{0}{S}_k$$

Since $\overset{0}{S}_k = T_{ka} Q_a$, the stress-to-load relationship becomes

$$S_i = S_{ia} Q_a \quad (33)$$

where S_{ia} is the stress-to-load matrix given by the operational sequence

$$S_{ia} = (\delta_{ik} - K_{ip} D_{pq}^{-1} H_{qk}) T_{ka} \quad (33a)$$

Note that $\delta_{ik} = 1$, when $i = k$, otherwise $\delta_{ik} = 0$

3. Displacement-to-load matrix Z_{ab}

Since the stresses are known in terms of the applied loads, it is possible to express strain energy in terms of these loads. On substitution,

$$V = \frac{1}{2} Q_a S_{ai} C_{ik} S_{kb} Q_b$$

Expression

$$Z_{ab} = S_{ai} C_{ik} S_{kb}$$

is the displacement-to-load matrix and strain energy is written in terms of the applied loads:

$$V = \frac{1}{2} Q_a Z_{ab} Q_b \quad (34)$$

By the first theorem of Castigliano, the displacement at any point a is given by

$$\partial V / \partial Q_a = z_a = Z_{ab} Q_b \quad (35)$$

When working with an automatic digital computer, determination of Z_{ab} is straightforward. Another expression for Z_{ab} is derived now which has the advantage of being a little more time saving and of permitting some numerical check on operations performed.

From the strain energy written in the form

$$V = \frac{1}{2} S_i C_{ik} S_k + F_p H_{pk} S_k + \frac{1}{2} F_p D_{pq} F_q$$

subtract, in view of equation (27)

$$\frac{1}{2} F_p (H_{pk} S_k + D_{pq} F_q) = 0$$

Thus

$$V = \frac{1}{2} S_i C_{ik} S_k + \frac{1}{2} F_p H_{pk} S_k \quad (36)$$

Remembering $H_{pk} = K_{pi} C_{ik}$ the above is brought to the form

$$V = \frac{1}{2}(\dot{S}_1 + F_p K_{p1}) \cdot C_{1k} \dot{S}_k = \frac{1}{2} S_1 C_{1k} \dot{S}_k$$

Because of the symmetry of C_{1k}

$$V = \frac{1}{2} \dot{Q}_a^T C_{ai} S_{ik} \dot{Q}_b$$

Hence

$$Z_{ab} = T_{ai} C_{ik} S_{kb} \quad (37)$$

is the alternative form of the displacement-to-load matrix. Apparently this form saves the cost of rearranging S_{ia} to S_{ai} and provides an important check, since the matrix Z_{ab} must be symmetric.

to p.37

*) It follows that rows and columns of non symmetric square matrices should not be designated by letters belonging to the same group. This restriction is quite meaningless and has not been observed in the text. See (33a) matrix

$$K_{ip} D_{pq}^{-1} H_{qk}$$

IV NUMERICAL EXAMPLES.

The methods of analysis presented above were checked on several numerical examples and compared with the test results. The considered problems subdivide into three categories:

1. Small illustrative problems analyzed by means of table computers.
2. A pilot problem solved on a standard I.B.M. punchcard machine.
3. A large scale computation.

1) Small Problems

Problems of this category were designed in order to check how the method behaves in practice and how it accounts for the wing sweep back, for torsional warping, and for shear lag effects. The computations were kept as simple as possible. Some results are quoted.

Fig. 12 represents one straight and one swept wing plate. There are four spars and three ribs. The fourth rib is rigid and is part of the support where all four spars are clamped. Computation involves

Stress points:	On spars	12
	On ribs	6
	On panels	<u>9</u>

$$\text{Hence } i = 27$$

$$\text{Redundant warping groups } p = 15$$

Terms containing Poisson's ratio were omitted in the energy formula. The curves a, b, c represent the spar flange stress at the clamped root. In particular:

- a) Curve (a) represents spar stress due to the bending effect of two loads $Q/2$ applied at the corners of the box as shown in Fig. 17. The bending stress is not the same for all spars on account of the flexibility of the ribs, in particular of the end rib where the load is applied.
- b) Curve (b) represents spar bending stress due to torsion applied by two loads $\pm Q/2$ at the corners of the box. This is the torsional warping stress.
- c) Curve (c) represents spar stress due to the bending effect of two loads $Q/2$ applied at the corners of the 30° swept box. An appreciable stress concentration exists at the root of the rear spar. Since the statically determinate part of stress distribution is the same as in the case of the curve (a), it follows that the stress concentration is detected only because the term $\sin \gamma \tau_{xy}(\sigma_x + \sigma_y)$ has been introduced in the energy formula.

Example of Figure 1. has been selected in order to investigate the shear lag effect. If lumping is done by existing webs, the analysis cannot be very accurate. Only four stress points can be introduced, two on spars and two on panels, and only one redundant warping group on the internal web. However, a quite fair stress distribution is obtained if nine planar groups are considered. In this case, by considering structural symmetry, we have

stress points:	On spars, real and fictitious,	15
	On ribs,	12
	On panels	12
		<hr/>

Hence $i = 39$

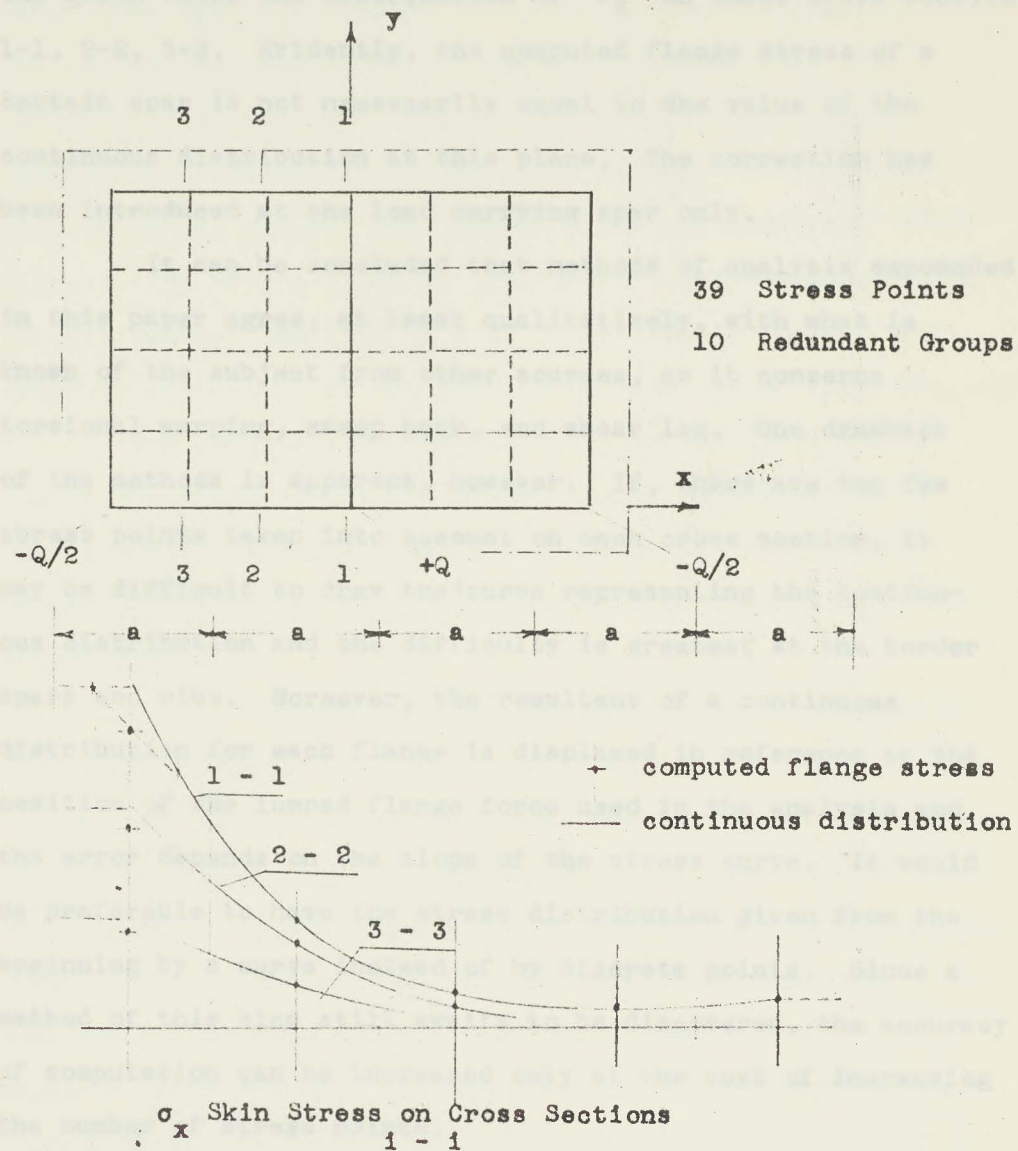


Fig. 18

Then redundant warping groups
redundant planar groups

1
9

Hence

$p = 10$

The graph shows the distribution of σ_x on three cross section, 1-1, 2-2, 3-3. Evidently, the computed flange stress of a certain spar is not necessarily equal to the value of the continuous distribution at this place. The correction has been introduced at the load carrying spar only.

It can be concluded that methods of analysis expounded in this paper agree, at least qualitatively, with what is known of the subject from other sources, as it concerns torsional warping, sweep back, and shear lag. One drawback of the methods is apparent, however. If, there are too few stress points taken into account on each cross section, it may be difficult to draw the curve representing the continuous distribution and the difficulty is greatest at the border spars and ribs. Moreover, the resultant of a continuous distribution for each flange is displaced in reference to the position of the lumped flange force used in the analysis and the error depends on the slope of the stress curve. It would be preferable to have the stress distribution given from the beginning by a curve instead of by discrete points. Since a method of this kind still awaits to be discovered, the accuracy of computation can be increased only at the cost of increasing the number of stress points.

2. Pilot Problem

It has been anticipated from the beginning that any

large scale analysis of a multi spar/rib structure is quite preposterous without a high speed digital computer. In order to check the method as to its applicability for automatic computation a problem indicated in fig. 19 was devised. The sketch represents, say, a dorsal fin plate built in elastically at the root. The loading consists of airloads applied perpendicularly to the plate at each spar/rib intersection and of moments and torques along the boundary. Their distribution may be given by preliminary considerations. The elastic support consists of a multi spar/plate so that each spar/rib connection at the root can rotate around the line F - F. The constraining moments may have any direction in the middle plane of the fin plate. Exact determination of the foundation stiffness being a problem for itself, for economy of time, the following approximate structure has been substituted.

It is assumed that the fin structure is extended so that quadrilateral cells are substituted for triangular ones. The support itself consists of four beams as shown in fig.20 and of inextensible links denoted by heavy lines. After the fin structure is connected with the support, the statically determinate stress is, for the most part, a simple beam bending as indicated in the text and is absorbed by the support as convenient. In order to make the support stress independent from the choice of the statically determinate system, it is assumed that six redundant warping groups act through faces, or webs, as marked previously by heavy lines.

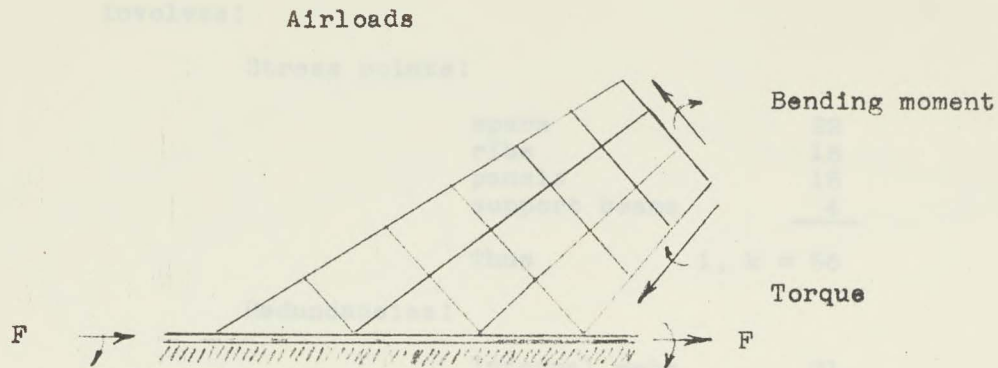


Fig. 19

Redundant groups
representing support

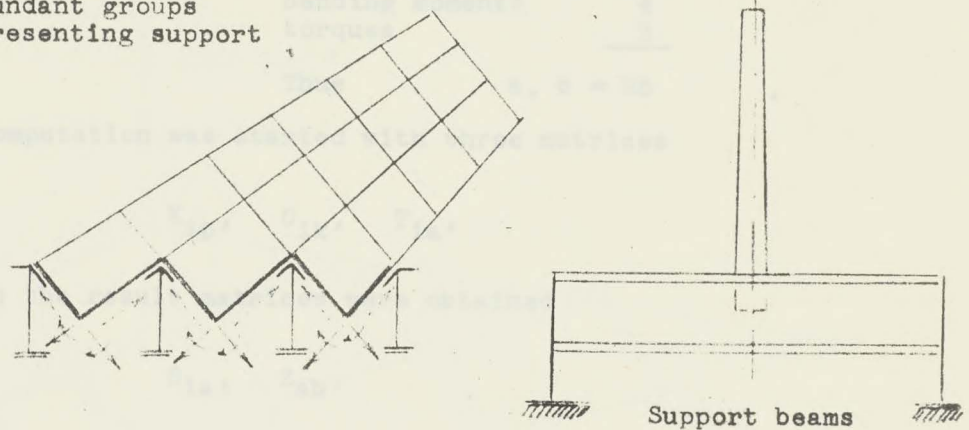


Fig. 20

These groups are connected with the support beams by means of the inextensible links. Thus one vector moment of each redundant group is displaced parallel to itself in the direction of the dotted arrow and resolved in two components, one

producing a beam bending, the other being assumed of no effect on deformation of the root rib or of the support.

The problem, when simplified as indicated above, involves:

Stress points:

spars	22
ribs	15
panels	15
support beams	<u>4</u>

Thus $i, k = 56$

Redundancies:

Internal webs	21
support	<u>6</u>

Thus $p, q = 27$

Load points:

airloads	18
bending moments	4
torques	<u>3</u>

Thus $a, b = 25$

The computation was started with three matrices

$$K_{ip}, C_{ik}, T_{ia},$$

and in the result matrices were obtained

$$S_{ia}, Z_{ab},$$

All work proceeded smoothly and was performed in one hundred hours of machine time. For some practical loading conditions the following results were obtained:

2. Large Scale Problem

The success of the pilot computation has prompted the decision to proceed with a large scale analysis. The considered structure is shown in Fig. 23. It consists of a

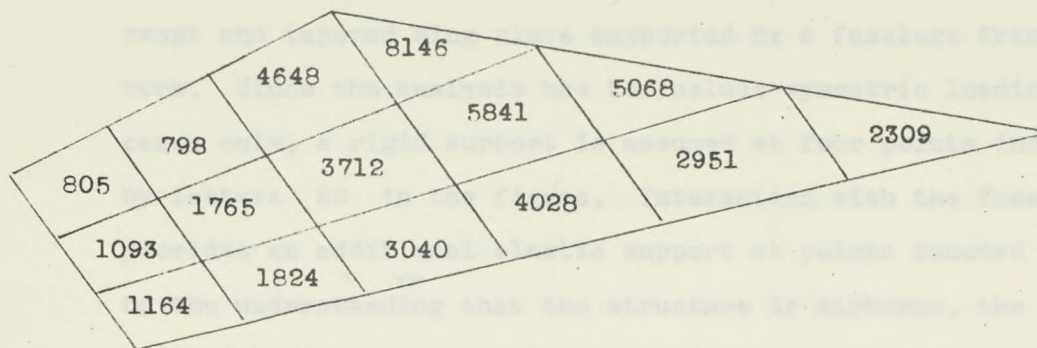


Fig. 23

Panel shearing stress τ_m psi.

local loads acting in these planes. Then the rigid support provides solely a means for measuring displacements.

72 independent loads are shown at intersections of

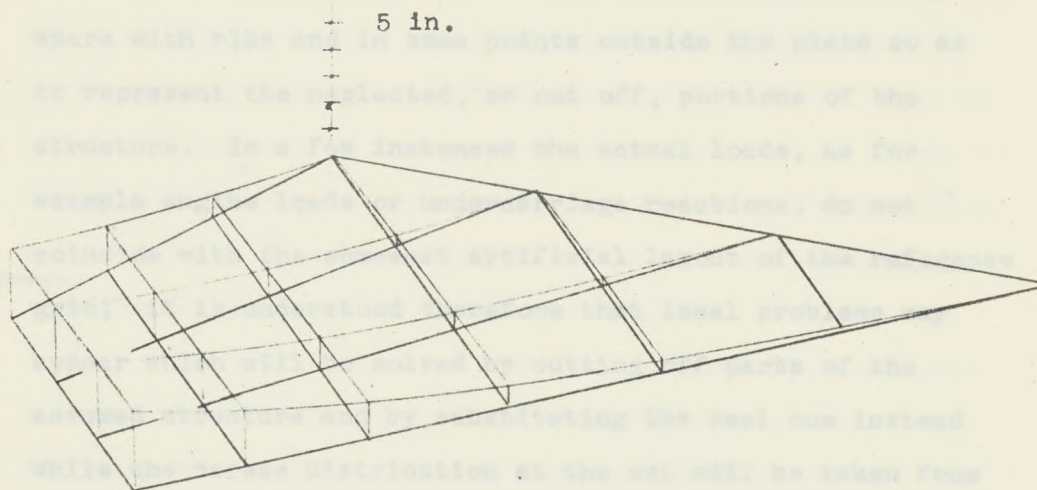


Fig. 24

— undeflected
— deflected structure

3. Large Scale Problem

The success of the Pilot Computation has prompted the decision to proceed with a large scale analysis. The considered structure is shown in Fig. 25. It consists of a swept and tapered wing plate supported by a fuselage framework. Since the analysis has to include symmetric loading cases only, a rigid support is assumed at four points indicated by letters RS in the figure. Interaction with the fuselage provides an additional elastic support at points denoted ES. On the understanding that the structure is airborne, the applied loads are supposed to be balanced always, so that the supporting rigid reactions are either nil or equal to the local loads acting in these places. Then the rigid support provides solely a datum for measuring displacements.

72 independent loads are chosen at intersections of spars with ribs and in some points outside the plate so as to represent the neglected, or cut off, portions of the structure. In a few instances the actual loads, as for example engine loads or undercarriage reactions, do not coincide with the somewhat artificial layout of the reference grid; it is understood therefore that local problems may appear which will be solved by cutting off parts of the assumed structure and by substituting the real one instead while the stress distribution at the cut will be taken from the main analysis.

The wing plate is 72 times redundant with MF warping groups placed on all internal walls. The connection

with the fuselage introduces three more redundant groups of the type MG and one redundant shearforce as indicated in Fig. 25. Altogether the structure is 76 times redundant.

Stress intensity is defined on 173 cross sections, which include all non zero spar and flange stresses and skin panel shears. The number of stress sections considered in the analysis is really much larger since many elements have been analyzed separately, and only the summaries have been incorporated in the main analysis.

Preparation of the numerical material took about 45 man-weeks. The following matrices were established:

C_{ik}	Matrix of	29,929	elements,	1,040	non zeros,
K_{ip}	Matrix of	13,148	elements,	370	non zeros,
T_{ia}	Matrix of	12,802	elements,	1,568	non zeros.

It should be noted that the above time figure did not include all preliminary work, i.e. assigning the proper structural cross sections, computing of effective widths and of elastic moduli. This part of the work was done by the Wing Groups of the Stress Office, who also established, from available data, a load Matrix Q_a^m composed of 72 columns of m elements representing airload and structural weight.

The computation contract was placed with the International Business Machines Company Ltd. in Toronto, Canada, and executed by the Scientific Computing Service in the New York Headquarters of the Company. Although all previous work has indicated that the undertaking is sound and reasonable, a great deal of uncertainty and risk was still involved.

The following questions could not be answered before the numbers were fed into the computer:

- 1) Is the $K_{pi}C_{ik}K_{kq}$ well conditioned for inversion?
- 2) Since any computed stress intensity is a difference of at least two large numbers representing groups, is it not likely that an overflow may occur or too many significant figures may be lost?
- 3) How many numerical errors are still in the basic matrices in spite of all checking and cross checking?
- 4) Are the computation facilities reliable enough to allow the handling of matrices of the order 173×173 .

The computation was brought to a successful end.

The following results were obtained:

- 1) Stress to Unit Load Matrix S_{ia} of 12,802 elements;
- 2) Displacement to Unit Load Matrix Z_{ab} of 5,184 elements;
- 3) S_1^m Matrix indicating Stress at 173 Cross Sections in m Loading Cases.
- 4) Z_a^m Matrix indicating Displacement at 72 Loading Points in m Loading Cases.

Figures 26, 27, 28, show a few interesting plots for the loading case corresponding to a large wing bending. Since at the present time, no comparison with experimental data is possible and no other exact computation exists, only a general examination of the results is presented:

- 1) On the evidence of the supplied arithmetic checks and of the continuity of the plotted curves, it is assumed that the computation is arithmetically correct. The checks were

provided by:

Symmetry of the D_{pq} Matrix,

Magnitude of the inversion error $D_{pq}^{-1} - \delta_{pq}$,

Symmetry of the Z_{ab} Matrix.

2) That the computation gives an adequate picture of the stress and displacement distribution can be seen from the following analysis:

- a) The chordwise bending at the centre line of the airplane is as expected. Fig. 27.
- b) There is no chordwise bending further outboard, but this is explained by the interference of the tip part. A correct twist of the wing is indicated, however.
- c) At the aircraft centre line the front spar is lifted up by the redundant shear force shown in Fig.25. This is indicated by the bending curves, Fig.26, and by reduction of bending stress, Fig.28.
- d) The maximum of the spar stress is shifted to the rear as expected. Fig. 28.

The computation gives no answer, however, as to the shearlag situation between the main spars and in this respect any experimental evidence can be quite valuable.

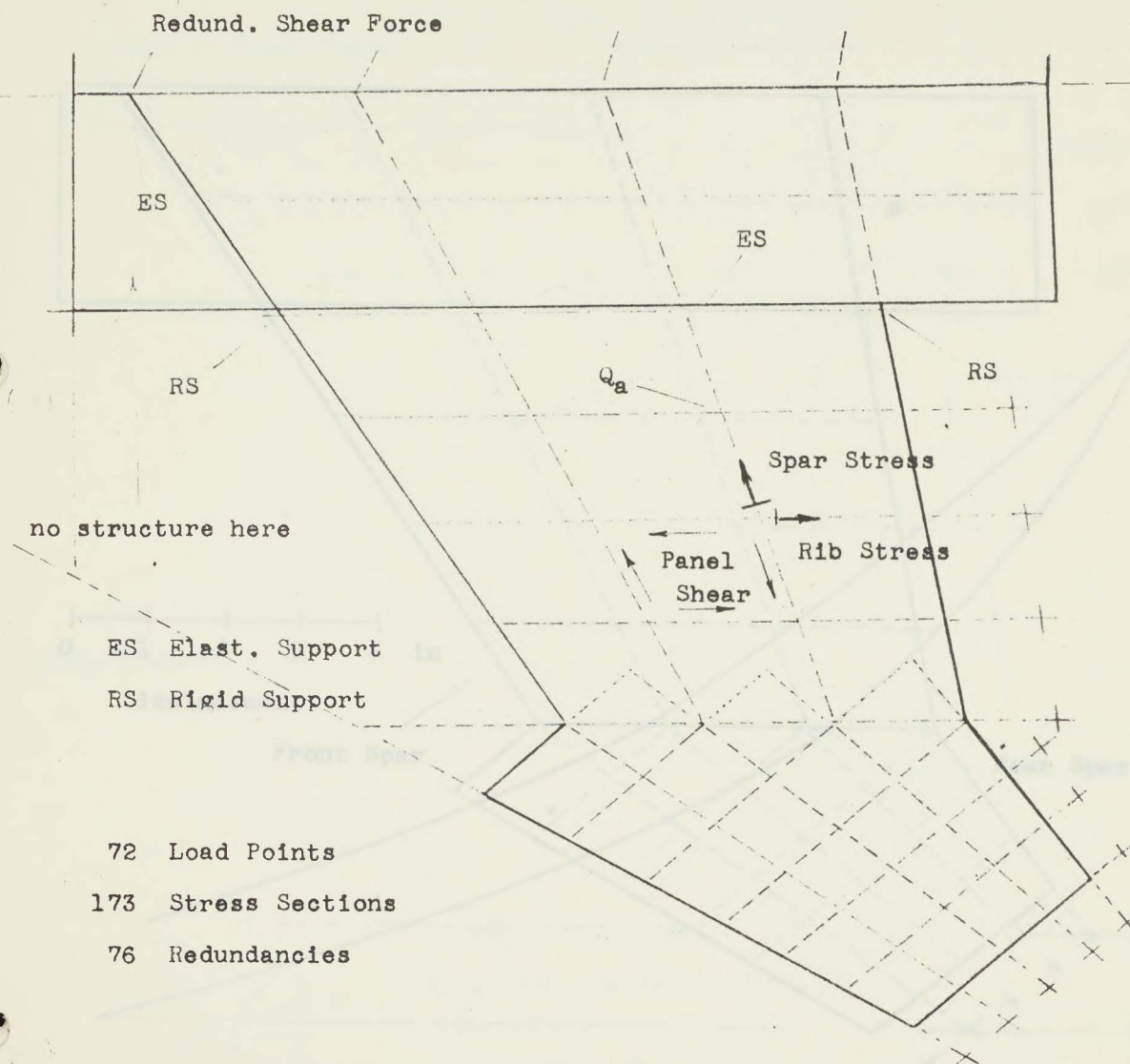
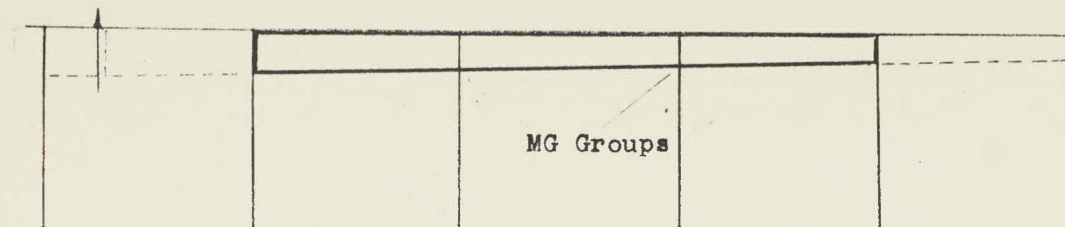
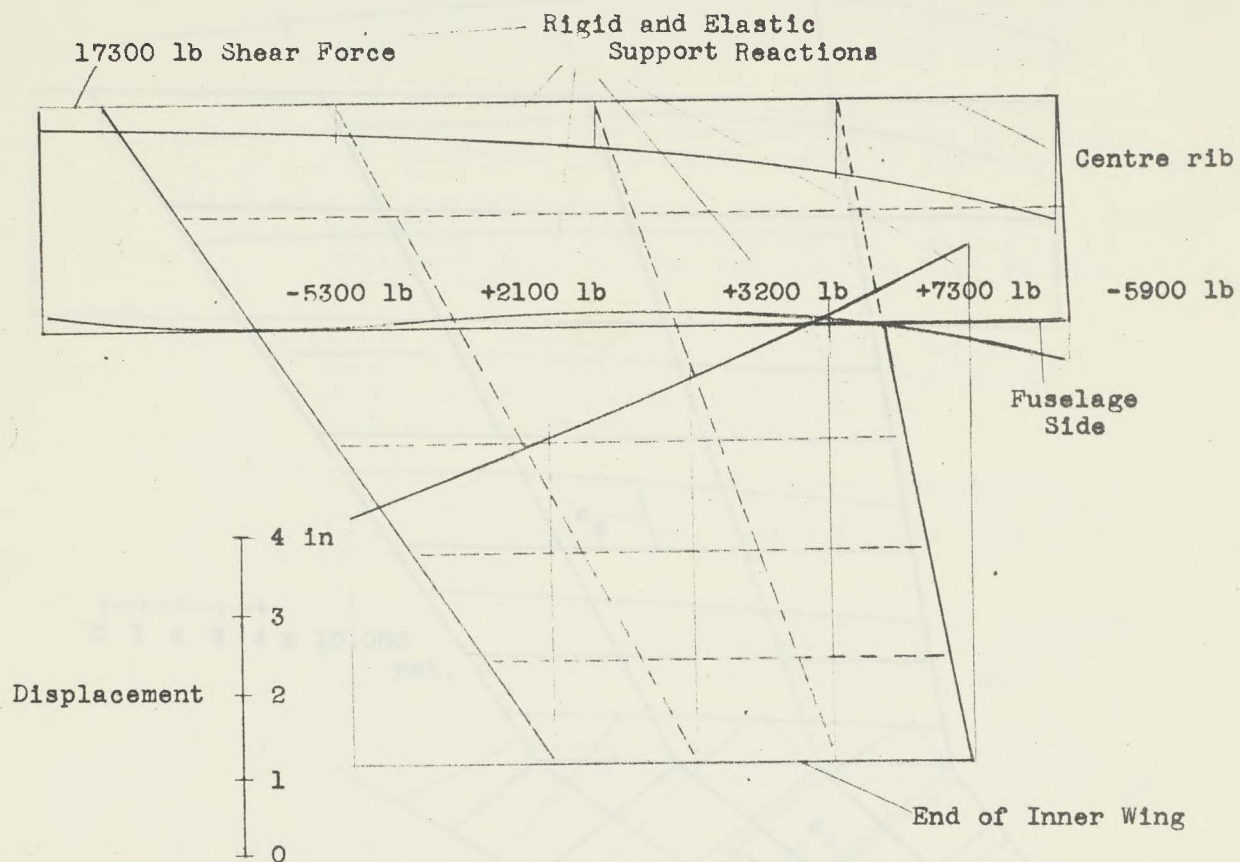


Fig. 25



Rib Displacement
Wing Fuselage Interaction

Fig. 27

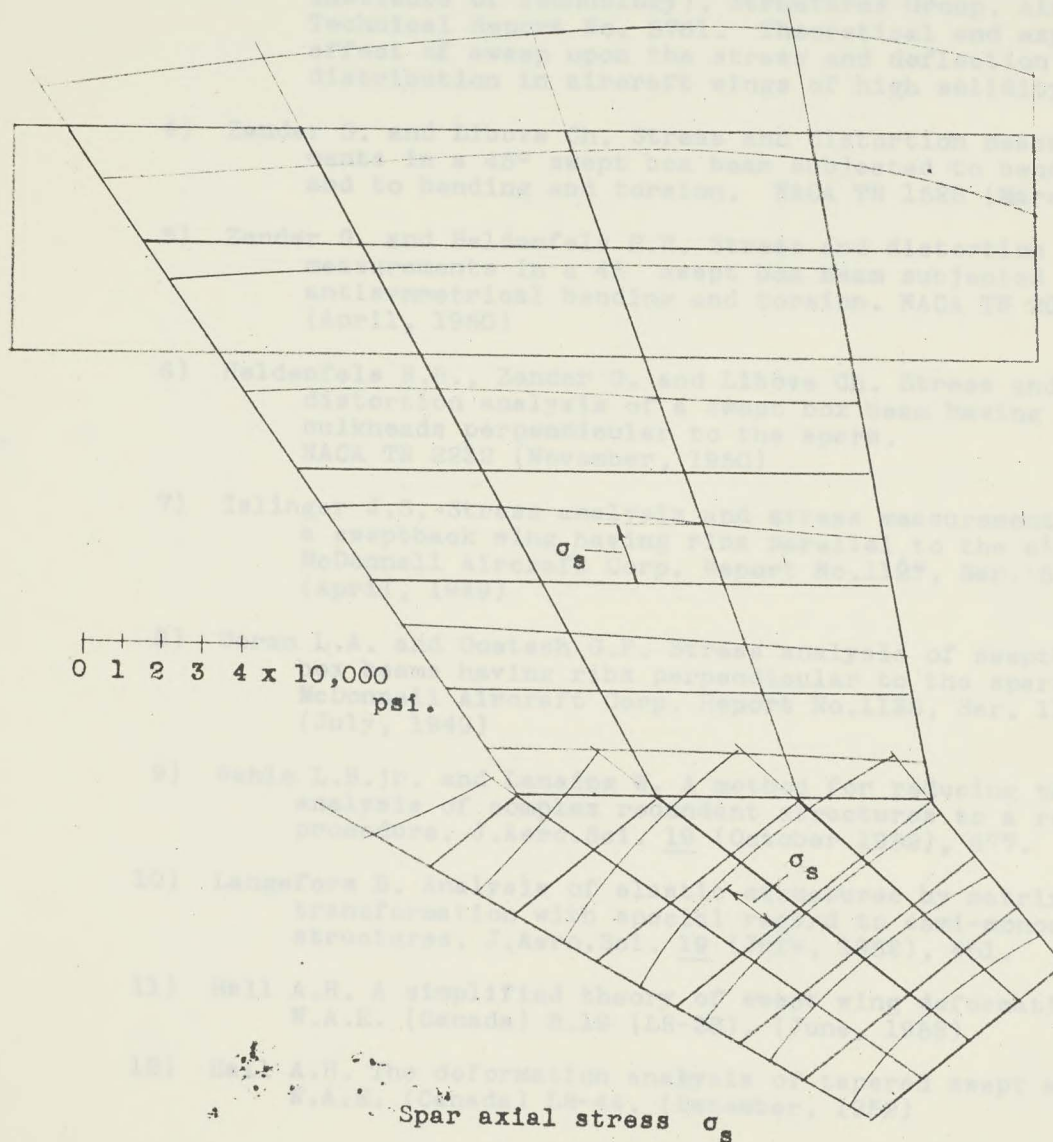


Fig. 28

REFERENCES

- 1) Levy S. Structural analysis and influence coefficients for delta wings. J.Aero.Sci. 20 (July, 1953), 449.
- 2) Fung Y.C. Bending of thin elastic plates of variable thickness. J.Aero.Sci. 20 (July, 1953), 455.
(= GALCIT Report No. 329)
- 3) GALCIT (= Guggenheim Aeronautical Laboratory, California Institute of Technology), Structures Group. Air Force Technical Report No. 5761. Theoretical and experimental effect of a sweep upon the stress and deflection distribution in aircraft wings of high solidity.
- 4) Zender G. and Libove Ch. Stress and distortion measurements in a 45° swept box beam subjected to bending and to bending and torsion. NACA TN 1525 (March, 1948)
- 5) Zender G. and Heldenfels R.R. Stress and distortion measurements in a 45° swept box beam subjected to antisymmetrical bending and torsion. NACA TN 2054 (April, 1950)
- 6) Heldenfels R.R., Zender G. and Libove Ch. Stress and distortion analysis of a swept box beam having bulkheads perpendicular to the spars. NACA TN 2232 (November, 1950)
- 7) Islinger J.S. Stress analysis and stress measurements for a sweptback wing having ribs parallel to the airstream. McDonnell Aircraft Corp. Report No. 1127, Ser. 16. (April, 1949)
- 8) Goran L.A. and Goetsch G.F. Stress analysis of sweptback box beams having ribs perpendicular to the spars. McDonnell Aircraft Corp. Report No. 1128, Ser. 11. (July, 1949)
- 9) Wehle L.B. jr. and Lansing W. A method for reducing the analysis of complex redundant structures to a routine procedure. J.Aero.Sci. 19 (October 1952), 677.
- 10) Langefors B. Analysis of elastic structures by matrix transformation with special regard to semi-monocoque structures. J.Aero.Sci. 19 (July, 1952), 451.
- 11) Hall A.H. A simplified theory of swept wing deformation. N.A.E. (Canada) R.19 (LR-28). (June, 1952)
- 12) Hall A.H. The deformation analysis of tapered swept wings. N.A.E. (Canada) LR-44. (December, 1952)

ACKNOWLEDGEMENT

The writer is indebted to Avro Aircraft Limited for allowing the publication of the material contained in this paper. The work was performed as a part of the regular stress analysis of a prototype under the supervision of Mr. F. P. Mitchell, Chief Stress Engineer, who outlined the scope of the undertaking and supported it by every means at his disposal. The writer has appreciated the cooperation of Mr. R. N. Shearly who performed most of the arithmetic work on the preliminary problems, on the oblique boundary condition, and without his skill and patience many theoretical relationships would never have been cleared and understood. Preparation of the numerical material for the computer techniques was in the hands of Messrs. A. C. Cominsky, R. N. Shearly, and D. L. Turner. Computations of the Pilot Problem were performed by the Computing Section of the company under^d Mr. R. Dowding. The large scale computation was carried out in the Scientific Computing Service of International Business Machines Co. Ltd. in New York. Mr. E. Kosko, Assistant Chief Stress Engineer was kind enough to review the text, and to make many remarks which were subsequently incorporated. He also helped in compiling the list of references.

1. EQUATIONS of EQUILIBRIUM for stress components in trapezoidal coordinates.

V APPENDIX

Chap. II, 2. Forces are now projected on the x , y , z , axes, and on the η axis.

1. Equations of equilibrium for stress components in trapezoidal coordinates.
2. Weighted averages for trapezoidal panels.
3. Analysis of trapezoidal cells.
4. Oblique boundary condition.
5. A superfluous MG group.
6. Partitioning the problem.

Fig. 20

Projecting forces on the x axis

forces in the limit

$$\sigma_{xx} \Delta x (\tan \gamma_1 - \tan \gamma_2) \cos \frac{\eta^* + \eta_2}{2}$$

$$\frac{d(\sigma_{xx})}{dx} \frac{dx}{\cos \gamma}$$

$$= \sigma_{xx} \Delta x (\tan \gamma_1 - \tan \gamma_2) \cos \frac{\eta^* + \eta_2}{2}$$

$$\frac{d(\sigma_{xx})}{dx} \frac{dx}{\cos \gamma}$$

$$\left. \begin{aligned} \sigma_{xx} \Delta x (\tan \gamma_1 - \tan \gamma_2) \cos \frac{\eta^* + \eta_2}{2} \\ \sigma_{xx} \Delta x (\tan \gamma_1 - \tan \gamma_2) \cos \frac{\eta^* + \eta_2}{2} \end{aligned} \right\}$$

which becomes

$$\frac{d(\sigma_{xx})}{dx} + \frac{\sigma_{xx}}{\cos \gamma} \tan \gamma = 0$$

(20)

1. EQUATIONS of EQUILIBRIUM for stress components in trapezoidal coordinates.

The trapezoidal stress components were defined in Chap. II, 2. Forces are now projected on the x , i.e. u , axis, and on the y axis.

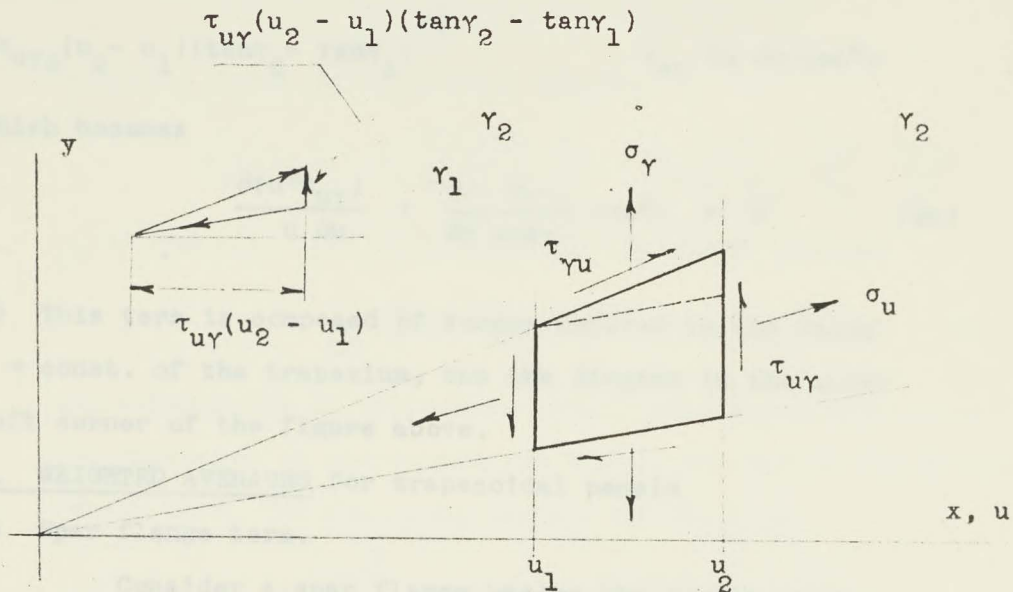


Fig. 29

Projecting forces on the x axis

yields in the limit

$$\left. \begin{aligned} & \sigma_{u2} u_2 (\tan \gamma_2 - \tan \gamma_1) \cos \frac{\gamma_1 + \gamma_2}{2} - \\ & - \sigma_{u1} u_1 (\tan \gamma_2 - \tan \gamma_1) \cos \frac{\gamma_1 + \gamma_2}{2} + \\ & + \tau_{u\gamma_2} (u_2 - u_1) \cos \gamma_2 / \cos \gamma_2 - \\ & - \tau_{u\gamma_1} (u_2 - u_1) \cos \gamma_1 / \cos \gamma_1 \end{aligned} \right\}$$

$$\frac{\partial(u\sigma_u)}{\partial u} \frac{du}{\cos \gamma} \frac{d\gamma}{d\gamma}$$

$$\frac{\partial \tau_{u\gamma}}{\partial \gamma} du d\gamma$$

which becomes

$$\frac{\partial(u\sigma_u)}{\partial u} + \frac{\partial \tau_{u\gamma}}{\partial \gamma} \cos \gamma = 0 \quad (2a)$$

c) Evaluation of $[\sigma^2]$

The integral to be computed is

$$dV = - \frac{t}{E} (m \cos^2 \gamma - \sin^2 \gamma) \sigma_r \sigma_s u' du dt^* \quad (13a)$$

where $t^* = t \tan \gamma$

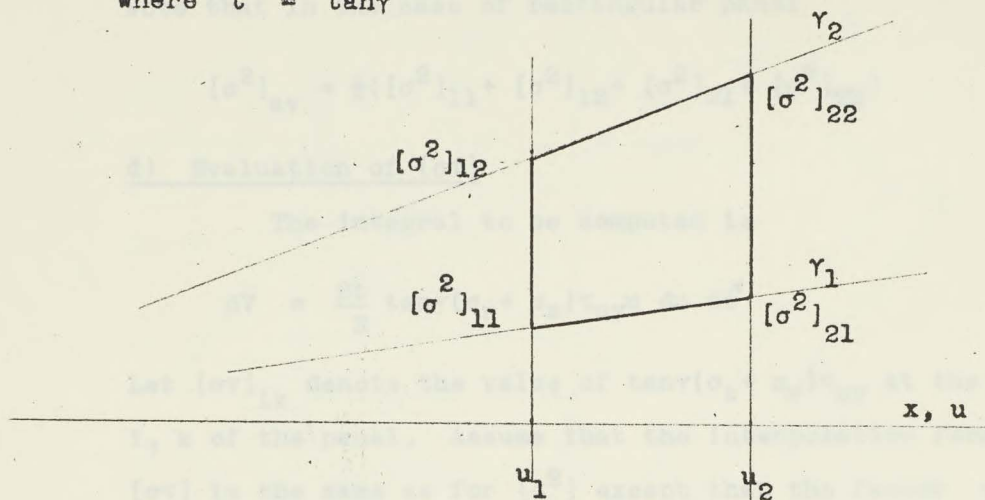


Fig. 31

Let $[\sigma^2]_{ik}$ denote the value of $(m \cos^2 \gamma - \sin^2 \gamma) \sigma_r \sigma_s$ at the corner i, k of the panel, see Fig. 27, and let us assume as an interpolation formula

$$[\sigma^2] = [\sigma^2]_{12} \frac{u_1}{u_2} \frac{u_2 - u}{u_2 - u_1} \frac{t^* - t_1^*}{t_2^* - t_1^*} + [\sigma^2]_{22} \frac{u_2}{u_1} \frac{u - u_1}{u_2 - u_1} \frac{t^* - t_1^*}{t_2^* - t_1^*} \frac{u_1 u_2}{u^2} +$$

$$+ [\sigma^2]_{11} \frac{u_1}{u_2} \frac{u_2 - u}{u_2 - u_1} \frac{t_2^* - t^*}{t_2^* - t_1^*} + [\sigma^2]_{21} \frac{u_2}{u_1} \frac{u - u_1}{u_2 - u_1} \frac{t_2^* - t^*}{t_2^* - t_1^*} \frac{u_1 u_2}{u^2}$$

where the factor $u_1 u_2 / u^2$ accounts for the variability of σ_s along the spar. After the integration is performed and the logarithmic terms are developed in series the following formula results

$$[\sigma^2]_{av} = ([\sigma^2]_{11} + [\sigma^2]_{12}) \left(1 - \frac{3u_2}{2(u_1 + u_2)}\right) + ([\sigma^2]_{21} + [\sigma^2]_{22}) \left(1 - \frac{3u_1}{2(u_1 + u_2)}\right) \quad (13b)$$

Note that in the case of rectangular panel

$$[\sigma^2]_{av} = \frac{1}{4}([\sigma^2]_{11} + [\sigma^2]_{12} + [\sigma^2]_{21} + [\sigma^2]_{22})$$

d) Evaluation of $[\sigma\tau]$

The integral to be computed is

$$dV = \frac{2t}{E} \tan\gamma(\sigma_r + \sigma_s) \tau_{uy} u \, du \, dt \quad (14a)$$

Let $[\sigma\tau]_{1k}$ denote the value of $\tan\gamma(\sigma_s + \sigma_r) \tau_{uy}$ at the corner 1, k of the panel. Assume that the interpolation formula for $[\sigma\tau]$ is the same as for $[\sigma^2]$ except that the factor $u_1 u_2 / u^2$ is squared to account for the variability of σ_s and τ_{uy} , composing the major part of the integrand. Then the following formula is obtained

$$[\sigma\tau]_{av} = \frac{u_1^2([\sigma\tau]_{11} + [\sigma\tau]_{12}) + u_2^2([\sigma\tau]_{21} + [\sigma\tau]_{22})}{2(u_1 + u_2)} \quad (14b)$$

In the case of a rectangular panel

$$[\sigma\tau]_{av} = \frac{1}{4}([\sigma\tau]_{11} + \dots)$$

3. ANALYSIS of TRAPEZOIDAL CELLS

Consider a cell represented in plan view by Fig.32.

Since the skin surface is a plane, the following holds:

$$h_{22}/x_2 = h_{12}/x_1, \quad h_{21}/x_2 = h_{11}/x_1.$$

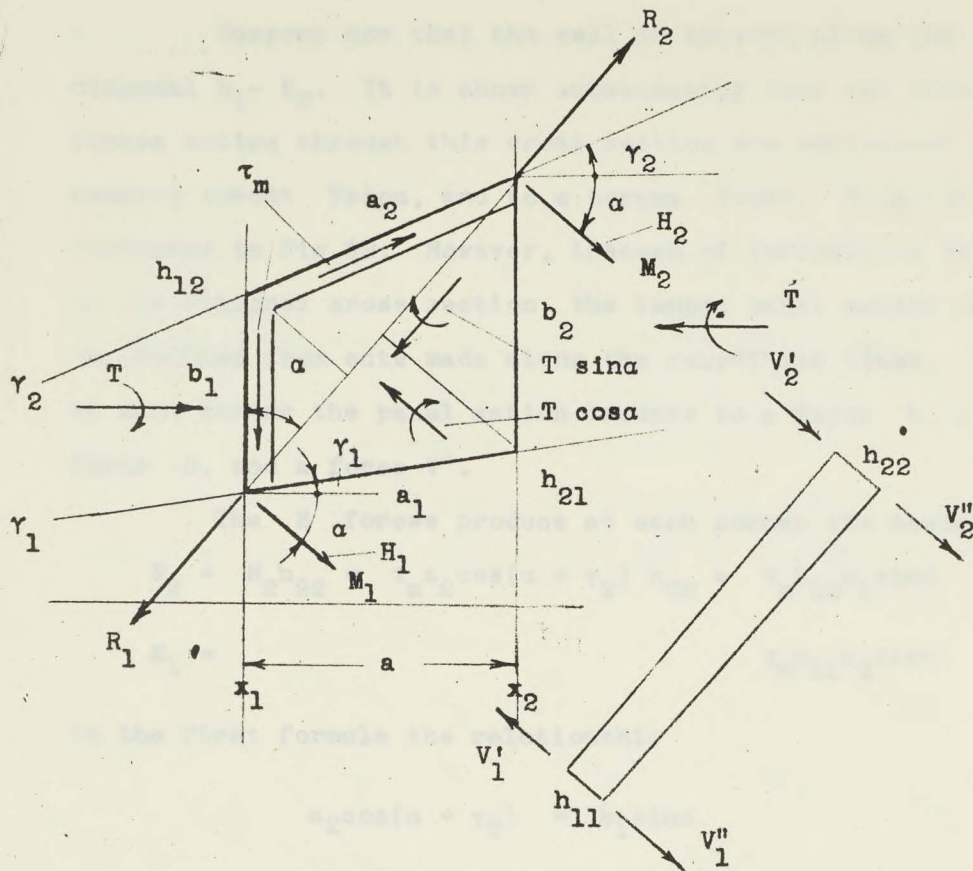


Fig. 32

It is assumed that the above ratios are very small quantities so that there is no need to distinguish between the panel and its projection as it concerns lengths and angles. The shearing stress of the panel is given by $\tau = \tau_m \frac{x_1 x_2}{x^2}$ (in this section τ lb/in.).

When the loading is a torque T , one obtains by the well known formula

$$\tau_1 = \tau_{m2}/x_1 = \frac{T}{(h_{12} + h_{11})b_1}$$

$$\tau_m = \frac{T}{h_{11}b_2 + h_{22}b_1}$$

(23)

Group MF_{u_1} . Assume that the flanges $\gamma = \text{const.}$ are extended up to their intersection point at the origin. Thus two beams are formed, a γ_2 -beam and a γ_1 -beam. Apply a down force F to the γ_2 -beam and an up F force to the γ_1 -beam. The flange forces S_{12} and S_{11} are given at once, and it is apparent that the panel shear τ_m can be obtained by considering the cell twisted by two couples of forces Q as indicated in Fig.33. The relation between the force F and the group bimoment is

$$F_{u_1} = MF_{u_1}$$

See Fig.34.

Group MF_{u_2} Apply first a negative group MF_{u_1} . Then transmit the flange forces from the face u_1 to the face u_2 as indicated in Fig. 34.

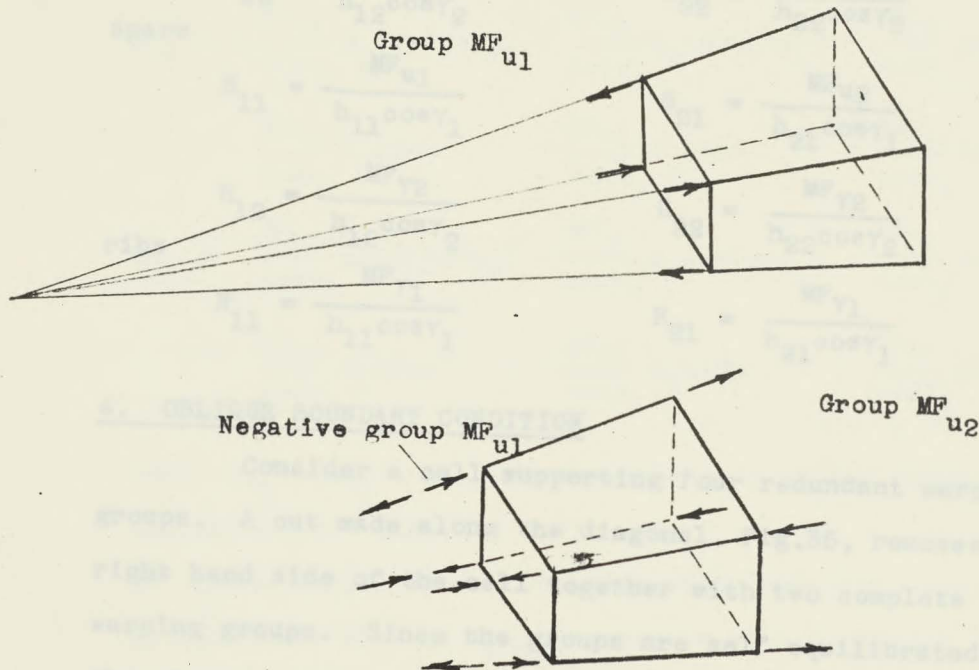


Fig. 34

The relation between the force F and the group bimoment is

$$F u_2 = M^F_{u2}$$

Groups $M^F_{\gamma 1}$ and $M^F_{\gamma 2}$. These groups should be considered as generated by torques having their vectors perpendicular to the faces $u = \text{const}$. The relation between the acting torque and the group bimoment is for the group 1 and 2 respectively,

$$T_{\gamma 1} \cos \gamma_1 = M^F_{\gamma 1}, \quad T_{\gamma 2} \cos \gamma_2 = M^F_{\gamma 2}$$

Then the following results are obtained:

$$\tau_m = \frac{M^F_{u2} b_1 - M^F_{u1} b_2 + M^F_{\gamma 2} a_2 - M^F_{\gamma 1} a_1}{a(h_{11} b_2 + h_{22} b_1)} \quad (15)$$

$$\begin{array}{l} \text{spars} \\ S_{12} = \frac{M^F_{u1}}{h_{12} \cos \gamma_2} \end{array} \quad \begin{array}{l} S_{22} = \frac{M^F_{u2}}{h_{22} \cos \gamma_2} \end{array} \quad (16)$$

$$S_{11} = -\frac{M^F_{u1}}{h_{11} \cos \gamma_1} \quad S_{21} = -\frac{M^F_{u2}}{h_{21} \cos \gamma_1}$$

$$\begin{array}{l} \text{ribs} \\ R_{12} = -\frac{M^F_{\gamma 2}}{h_{12} \cos \gamma_2} \end{array} \quad \begin{array}{l} R_{22} = \frac{M^F_{\gamma 2}}{h_{22} \cos \gamma_2} \end{array} \quad (17)$$

$$R_{11} = -\frac{M^F_{\gamma 1}}{h_{11} \cos \gamma_1} \quad R_{21} = \frac{M^F_{\gamma 1}}{h_{21} \cos \gamma_1}$$

4. OBLIQUE BOUNDARY CONDITION

Consider a cell supporting four redundant warping groups. A cut made along the diagonal, Fig.35, removes the right hand side of the cell together with two complete warping groups. Since the groups are self equilibrated, the stress system acting through the cross-section has no resultant. It produces, however, a distortion of the inboard

structure in a three fold way, see Main Text:

1) Components normal to the cross section, of the cut flange forces and of the panel action, generate a bimoment MH , This constitutes a warping group of the first kind applied to the next cell inboard. In particular:

at the point (2) the warping moment is

$$MH_2 = - M_2 + \text{Norm.components of } MF_{\gamma_2}, MF_{u_2},$$

at the point (1) the warping moment is

$$MH_1 = - M_1 + \text{Norm.components of } MF_{\gamma_1}, MF_{u_1}.$$

In the above, M_2 and M_1 stand for the lumped panel action due to τ_m ; the corresponding formulae have been derived in section 3 of this chapter, see (24) and Fig. 32. When written in full, the above expressions become:

$$\begin{aligned} MH_2 = & - \frac{MF_{u_2}}{\cos \gamma_2} m_2 \cos(\alpha + \gamma_2) + \frac{MF_{u_1}}{\cos \gamma_1} m_2 \cos(\alpha + \gamma_1) + \frac{MF_{u_2}}{\cos \gamma_2} \cos(\alpha + \gamma_2) \\ & - \frac{MF_{\gamma_2}}{\cos \gamma_2} m_2 \sin \alpha + \frac{MF_{\gamma_1}}{\cos \gamma_1} m_2 \sin \alpha + \frac{MF_{\gamma_2}}{\cos \gamma_2} \sin \alpha \\ MH_1 = & \frac{MF_{u_2}}{\cos \gamma_2} m_1 \cos(\alpha + \gamma_2) - \frac{MF_{u_1}}{\cos \gamma_1} m_1 \cos(\alpha + \gamma_1) + \frac{MF_{u_1}}{\cos \gamma_1} \cos(\alpha + \gamma_1) \\ & - \frac{MF_{\gamma_2}}{\cos \gamma_2} m_1 \sin \alpha - \frac{MF_{\gamma_1}}{\cos \gamma_1} m_1 \sin \alpha + \frac{MF_{\gamma_1}}{\cos \gamma_1} \sin \alpha \end{aligned}$$

Thus $MH_2 = MH_1 = MH$ and the existence of the bimoment is demonstrated. (25)

2) Shear forces of the cut webs (spar and rib), expressed by the terms such as $\tau_w h_{22}$, together with a portion of the diagonal shear force S produce a distorsion of the cross section. As a rule, this action will be stopped by a rib

belonging to the "R" rib. Since, as it concerns this work,

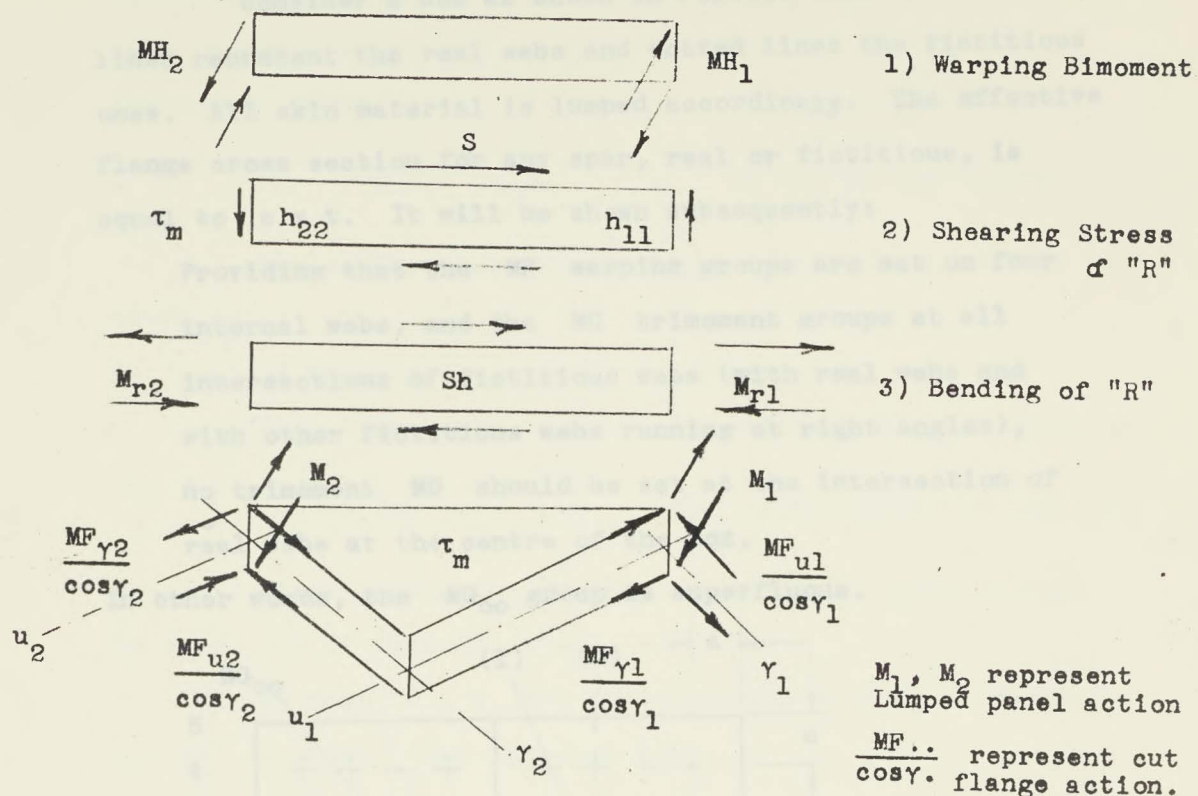


Fig. 35

all webs are assumed stiff in shear, the above action cannot be followed any further.

3) Components parallel to the cross section of the cut flange forces, produce a bending of the "R" rib. This is described by two bending moments: M_{r2} made of S-components of MF_{u2} and $MF_{\gamma2}$, M_{r1} made of S-components of MF_{u1} and $MF_{\gamma1}$, each of them being equilibrated by a portion of the moment Sh . Fig.35.

These moments generate stresses in the structure inboard as explained in the main text, Chap. II, 6. Thus the stress intensity at a particular grid point of "R" can be taken as an average of the action of the four warping groups. (26)

5. A SUPERFLUOUS MG GROUP

Consider a box as shown in Fig.36. Let the full lines represent the real webs and dotted lines the fictitious ones. All skin material is lumped accordingly. The effective flange cross section for any spar, real or fictitious, is equal to $a \times t$. It will be shown subsequently:

Providing that the MF warping groups are set on four internal webs, and the MG trimoment groups at all intersections of fictitious webs (with real webs and with other fictitious webs running at right angles), no trimoment MG should be set at the intersection of real webs at the centre of the box.

In other words, the MG_{00} group is superfluous.

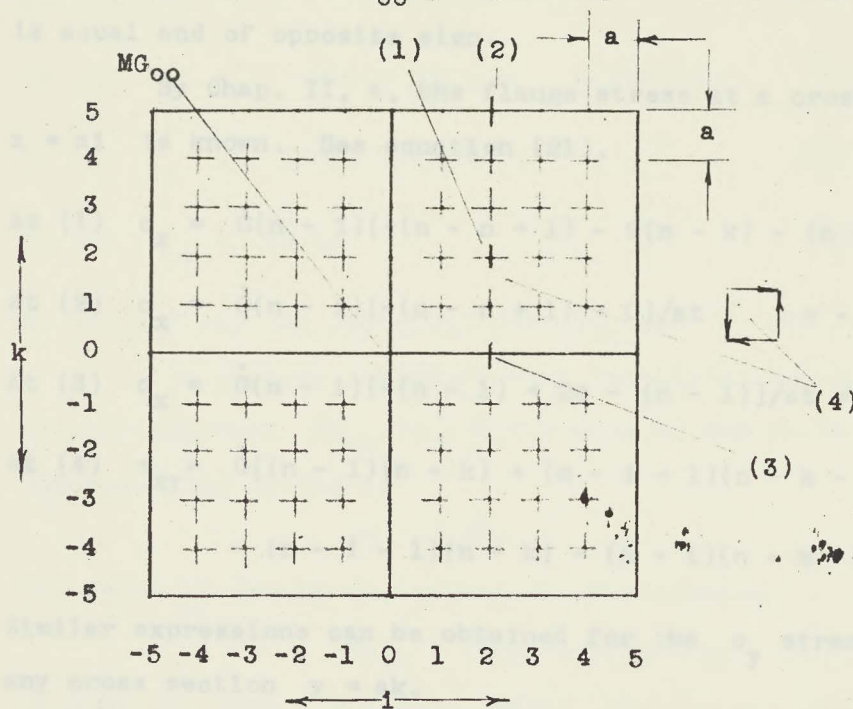


Fig. 36

Assume, for the sake of simplicity, that the box is of constant depth h . There are 6 real webs, and 16 fictitious webs in the figure where, also, the numbering system is explained. Thus

$$-n < \frac{i}{k} < n \quad (n = 5 \text{ in the figure})$$

Assume that the stress system of the upper surface is given by:

$$G_{ik} = \begin{cases} \begin{array}{ll} i \text{ negative} & i \text{ positive} \\ \dot{G}(n+1)(n-k), & = \dot{G}(n-1)(n-k), \quad k \text{ positive} \\ \dot{G}(n+1)(n+k), & = \dot{G}(n-1)(n+k), \quad k \text{ negative} \end{array} \end{cases}$$

where \dot{G} is a constant. Stress system of the lower surface is equal and of opposite sign.

By Chap. II, 4, the flange stress at a cross section $x = ai$ is known. See equation (21).

$$\text{At (1)} \quad \sigma_x = \dot{G}(n-1)[-(n-n+1) - 2(n-k) - (n-k-1)]/at = 0$$

$$\text{At (2)} \quad \sigma_x = \dot{G}(n-1)[-(n-n+1) + 0]/at = -\dot{G}(n-1)/at$$

$$\text{At (3)} \quad \sigma_x = \dot{G}(n-1)[-(n-1) + 2n - (n-1)]/at = 2\dot{G}(n-1)/at$$

$$\begin{aligned} \text{At (4)} \quad \tau_{xy} = & \dot{G}[(n-1)(n-k) + (n-1-1)(n-k-1) - \\ & - (n-1-1)(n-k) - (n-1)(n-k-1)]/at = \dot{G}/at \end{aligned}$$

Similar expressions can be obtained for the σ_y stress at any cross section $y = ak$.

On the other hand, consider a simple Airy group

$$G = n\dot{G}$$

within the assembly of Fig. 37.

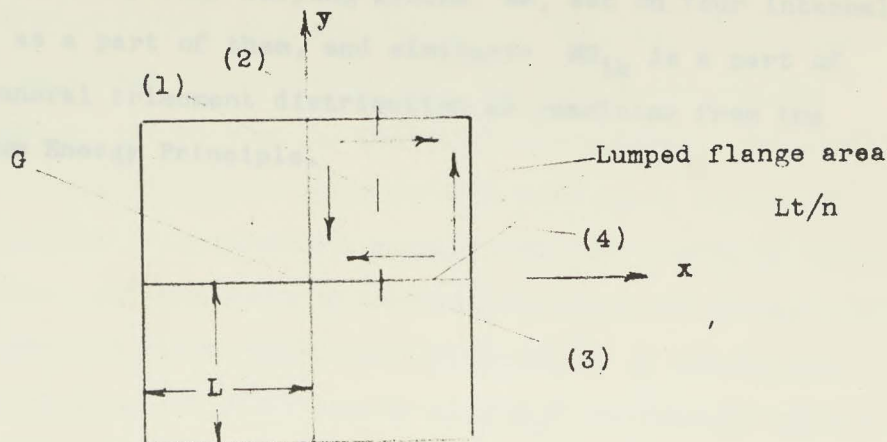


Fig. 37

This group produces the following stress distribution:

At (1) $\sigma_x = 0$ by definition.

At (2) $\sigma_x = -n\dot{G}(1 - x/L)/at$ equivalent $-\dot{G}(n - 1)/at$

At (3) $\sigma_x = 2n\dot{G}(1 - x/L)/at$ " $2\dot{G}(n - 1)/at$

At (4) $\tau_{xy} = n\dot{G}/Lt$ " \dot{G}/at

As one can see the distributions G_{ik} and G are identical.

It appears therefore that the stress corresponding to the trimoment MG_{00} is a difference of two stress distributions. One is due to

$$MG = n\dot{G}h$$

the other is due to the trimoment distribution

$$MG_{ik} = \dot{G}_h(n - 1)(n - k) \text{ etc.}$$

without the term $i = k = 0$. Hence MG_{00} is not an independent variable. In the course of computation MG_{00} is

represented by four warping groups MP , set on four internal webs, as a part of them, and similarly MG_{1k} is a part of the general trimoment distribution as resulting from the Minimum Energy Principle.

6. PARTITIONING the PROBLEM

When analysing a multi redundant structure it is sometimes expedient to subdivide the task into a few smaller problems as can be seen on the following example. Suppose that the main structure consists of three parts connected in a statically determinate manner, each part being 10 times redundant. If the whole structure were analysed in one block the number of punch-cards used in inversion of the elastic matrix is about 27,000; but if each part is treated separately the number of cards is only 3,000. As a rule partitioning of a problem should be undertaken only if the redundant link is weak and if the number of partial problems is not large, since with modern high speed digital computers, as it concerns time spent on computation, the size of matrices matters less than the inconvenience of input and output of data. Therefore, if partitioning involves frequent reading out of data and extensive handling of magnetic tapes, it may be faster to proceed without partitioning. On the other hand, partitioning may be advantageous if some parts of the structure are expected to change or to occur in variants. Then, incorporation of changes may be done with little cost.

In establishing partition boundaries and redundancies, it is necessary to distinguish between a simply connected structure and a multiply connected one. Suppose that the structure is built up in the following way: There is a structural part, the base connected with the foundation. This part supports other parts which carry other parts, and so on. If no other connections exist between parts as those

explained, the structure resembles a tree and is called a simply connected redundant structure. In this case, the connections, of the base with the foundation, of the parts with each other, although statically indeterminate in general, are such that the corresponding redundancies affect directly two adjacent parts only. These redundancies are denoted here as border redundancies, in opposition to the internal redundancies which are supposed to be eliminated in the first step of computation. In a simply connected structure there is never any doubt which load path leads to the foundation.

If the structure possesses other connections, as if some branches of a tree were grown together, it is called a multiply connected structure. In this case, redundancies exist which affect several parts forming a closed circuit. Subsequently they are referred to as closed circuit redundancies. In a multiply connected structure, it is, in general, ambiguous which load path leads to the foundation. Some information on stress systems in multi connected bodies can be obtained from S. Timoshenko's Theory of Elasticity, par.39, p. 120, (Ed. 1951).

There is no difficulty in establishing rules of partitioning. A portion of the structure is cut out and the statically determinate reactions and redundancies at the cuts are defined. Then the loads are introduced:

- a) The air and inertial loads applied to the part in question.
- b) The statically determinate action of the attached structure and the corresponding border redundancies if any.

- c) In a multiply connected structure, the closed circuit redundancies.

All these items are summarized as loads in general and the problem is solved for stress and displacement in the usual manner as indicated in Chapter III. In doing so the following matrices are obtained for any structural part:

stress to unit load	S_{ia}
displacement to unit load	Z_{ab}

Note that in the above the statically determinate reactions of a part do not appear as loads acting on the part. They appear as loads acting on the supporting structure; in other words, on parts situated farther down on the path to the foundation.

In order to combine the partial problems for final solution, a unified index and notation system is introduced for the whole structure. Accordingly:

- A) Loads Q_a of partial problems (acting loads, border and closed circuit redundancies) are denoted as fictitious stresses S_u ; index system u, v .
- B) These loads are expressed in terms of the remaining redundancies F_p by means of a matrix K_{up} ; index system p, q , and by means of
- C) the loads applied to the whole structure. These loads are denoted Q_a ; index system a, b . Here the indices a, b , have acquired a new meaning and run through all applied load numbers obtained when all partial problems are put together. The matrix relation is T_{ua} .

D) The overall strain energy matrix is built up consequently of all partial matrices Z_{ab} and is denoted C_{uv} . Thus the procedure of Chapter III can be applied, with index u written for i , and two new matrices can be obtained:

- 1) S_{ua} expressing all loads and all redundancies, treated as loads in partial problems, in terms of acting air and inertia loads.
- 2) Z_{uv} presenting the overall displacement matrix.

The overall stress to unit load matrix is evidently

$$S_{ia} = S_{iu} S_{ua}$$

where the index i runs through all stress points of the structure. The computations involved in the overall problem are rather simple due to the small numbers of unknowns and to the fact that the matrix T_{ua} is for the most part a unit matrix.

